Appendix C

Supplementary information for Chapter 4. NMR spectra, infrared spectra, HRMS isotopic pattern matching, X-ray cystallography details (pictures and hydrogen bond tables) and spectroscopic titration and fitting plots.

C.1. NMR spectra of ligands and complexes

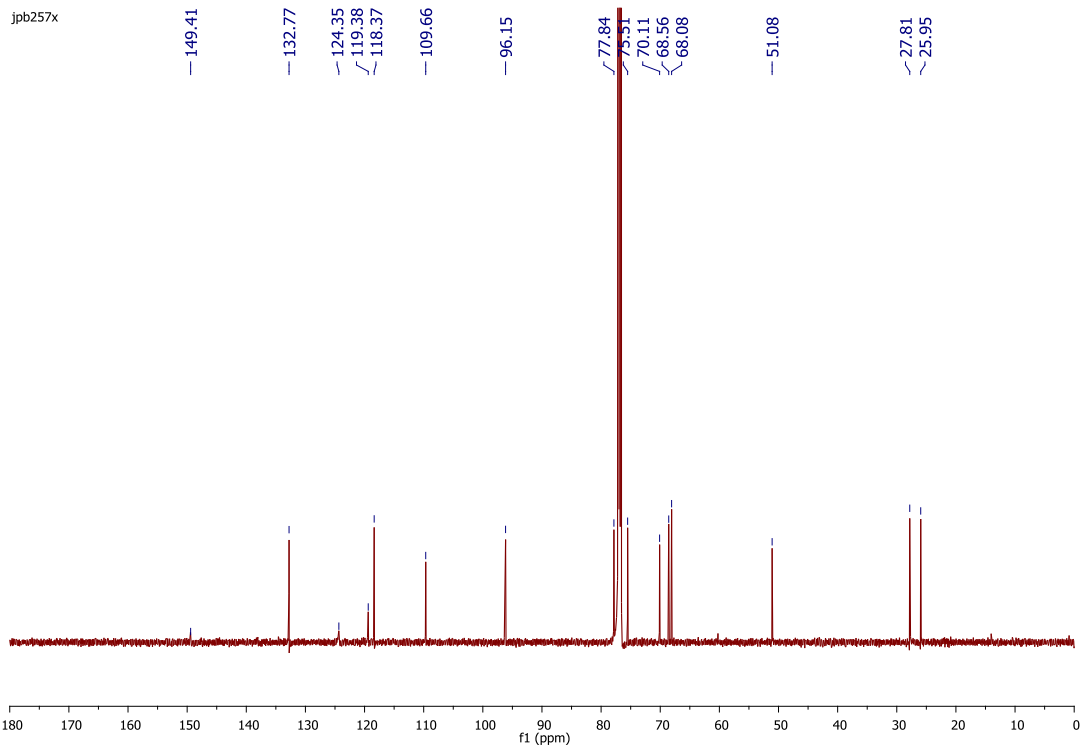

Figure C.1 ^{13}C NMR (150 MHz, $CDCl_3$) spectrum of **96**.

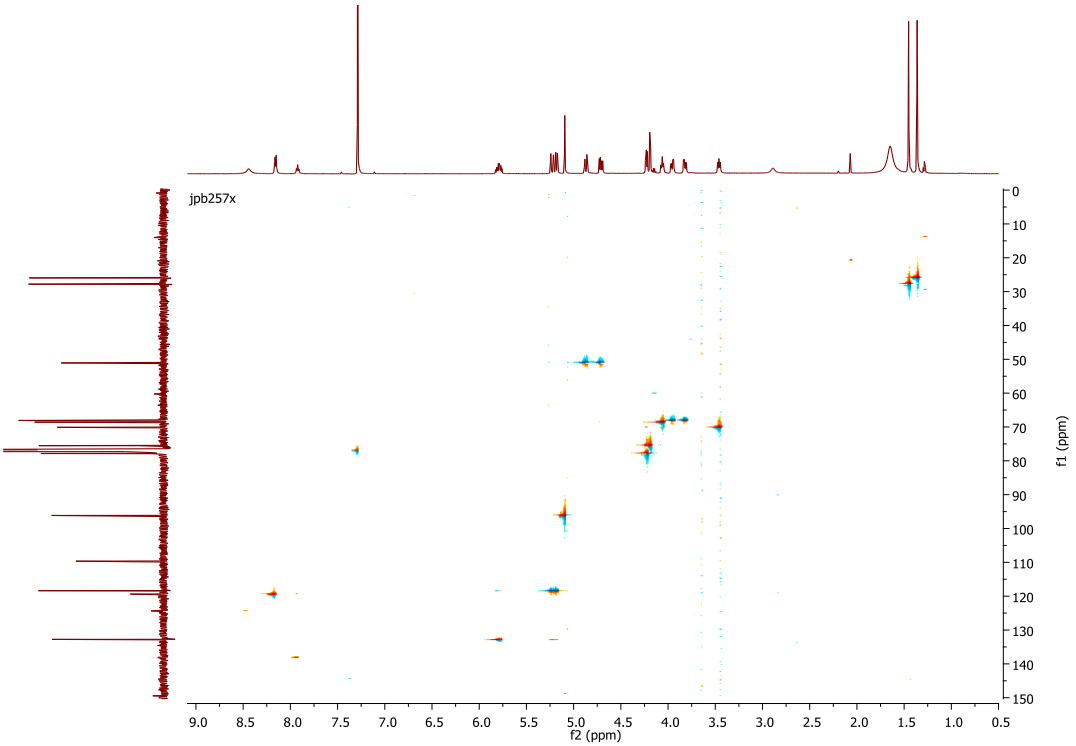

Figure C.2 HSQC of ligand **96**.

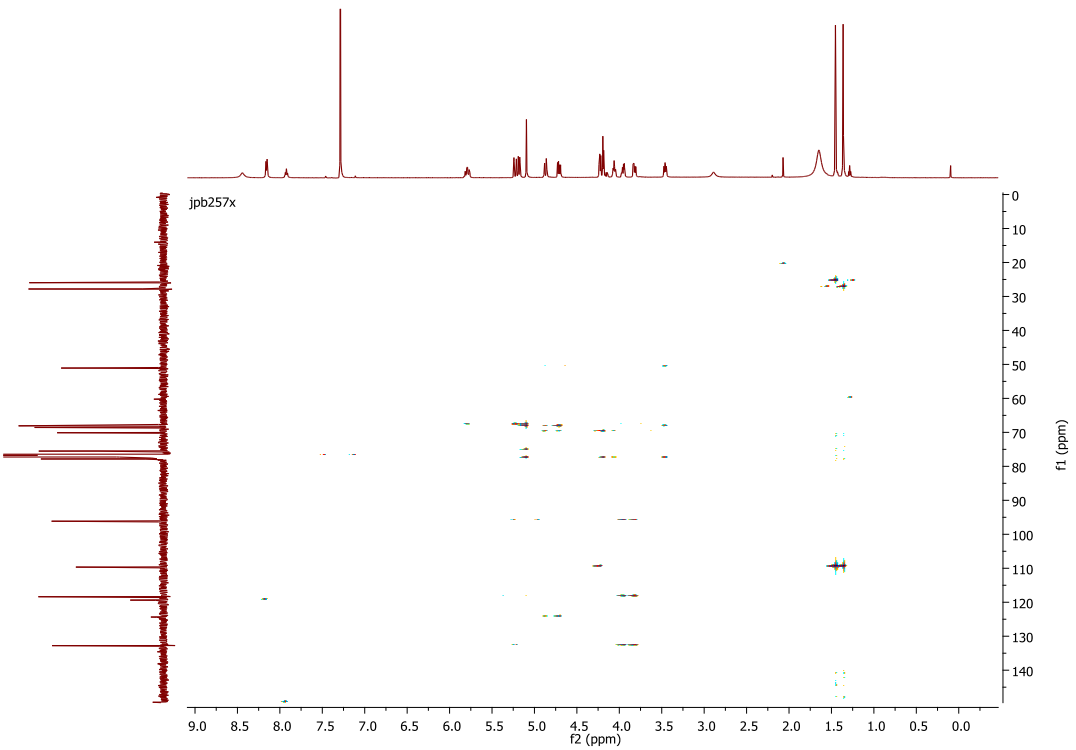

Figure C.3 HMBC of ligand **96**.

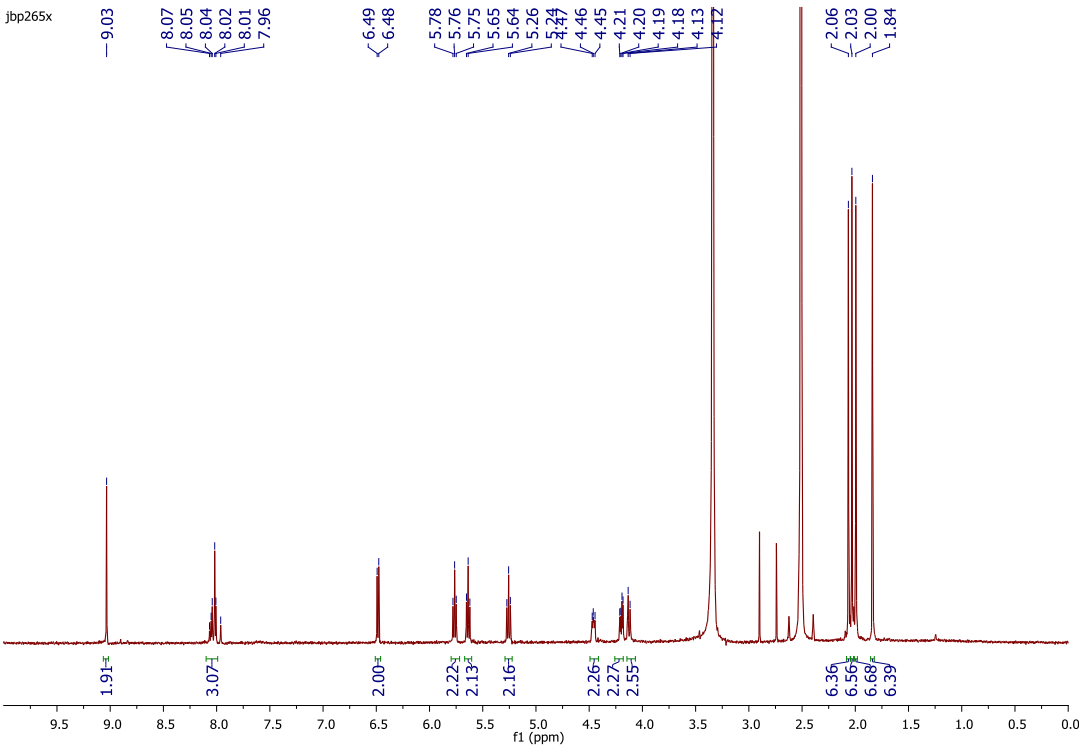

Figure C.4 ^{1}H NMR (600 MHz, DMSO-d_6) spectrum of **97**.

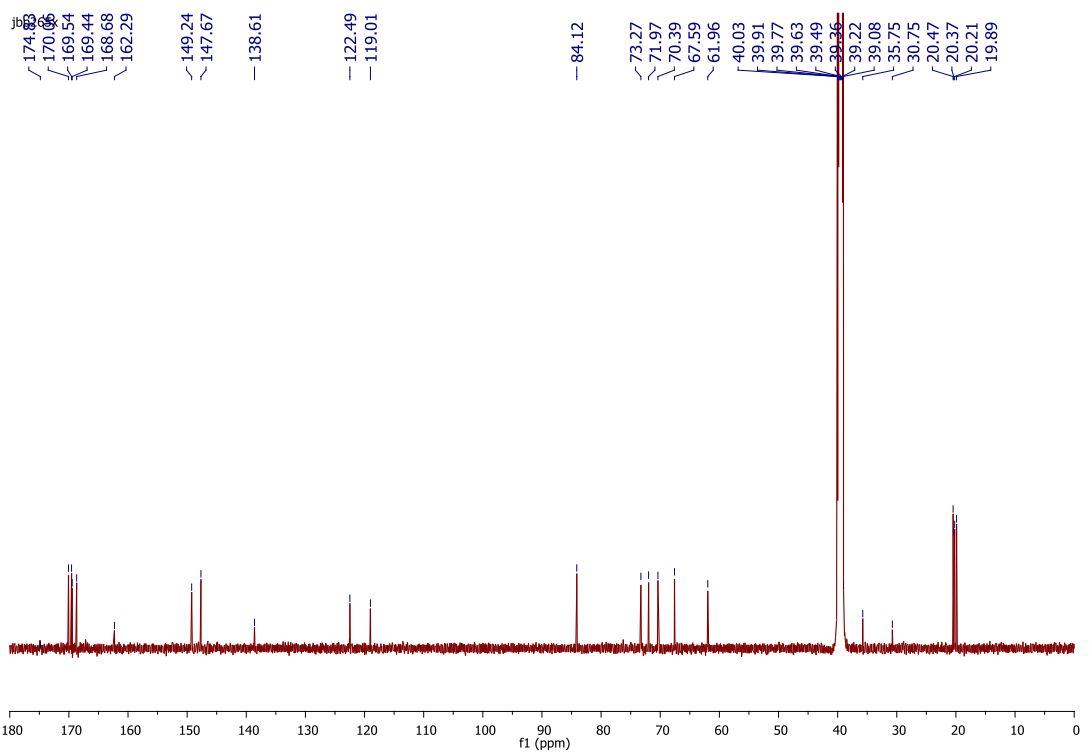

Figure C.5 ^{13}C NMR (150 MHz, DMSO-d_6) spectrum of **97**.

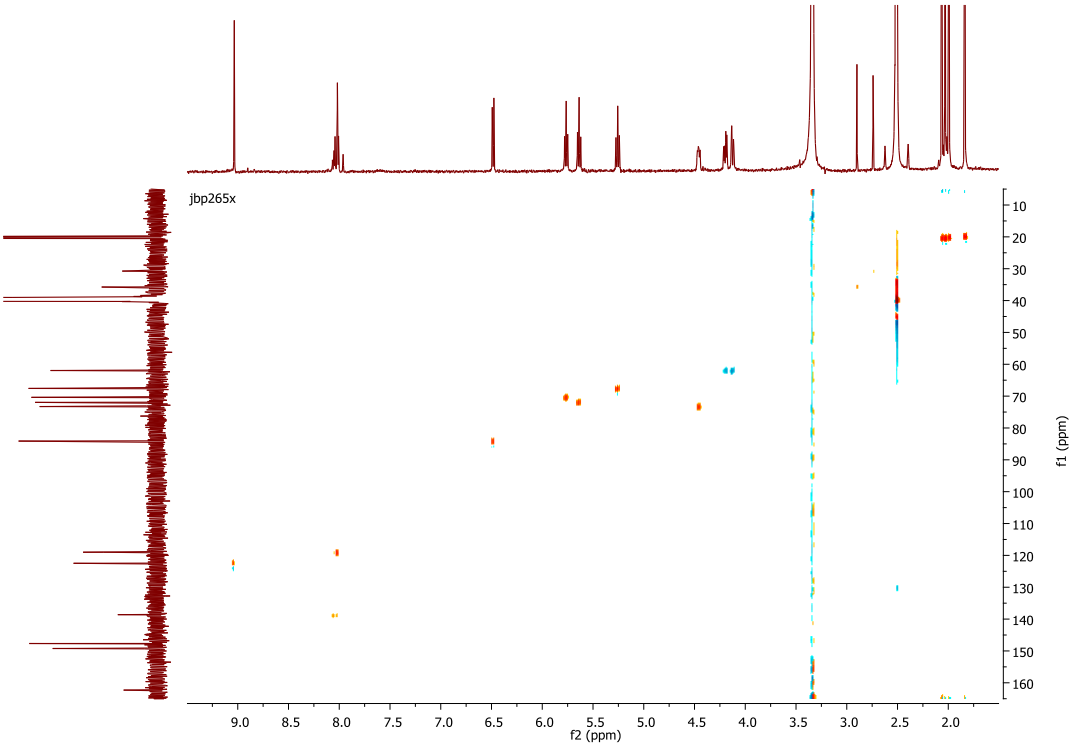

Figure C.6 HSQC of ligand **97**.

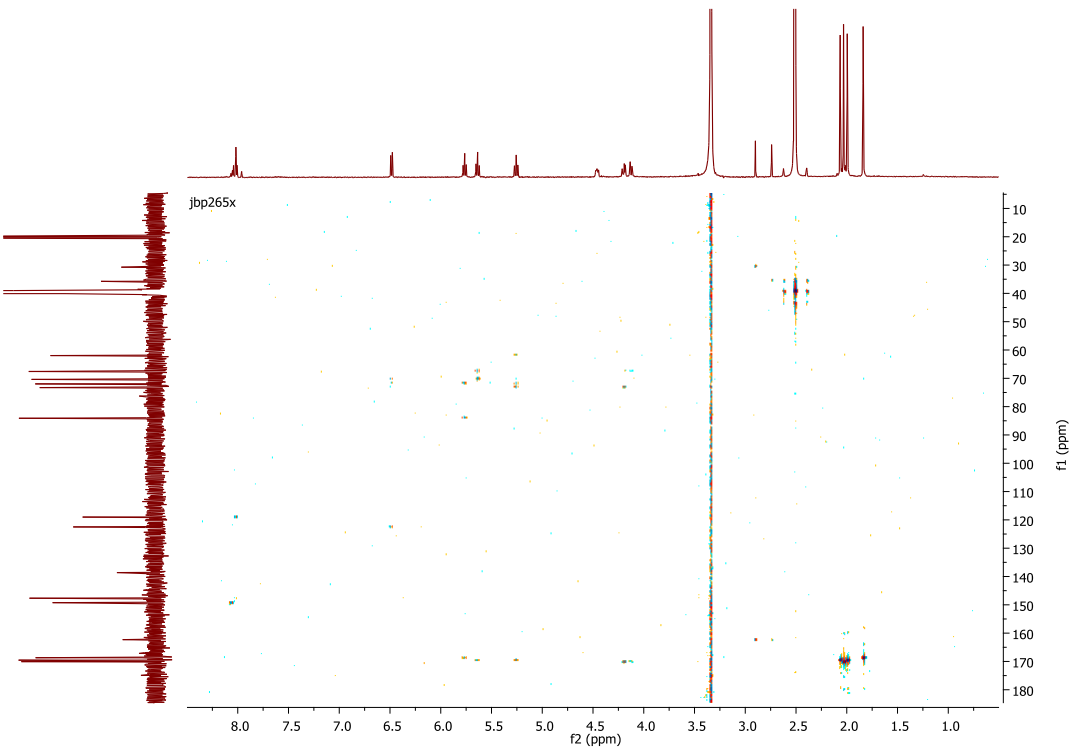

Figure C.7 HMBC of ligand **97**.

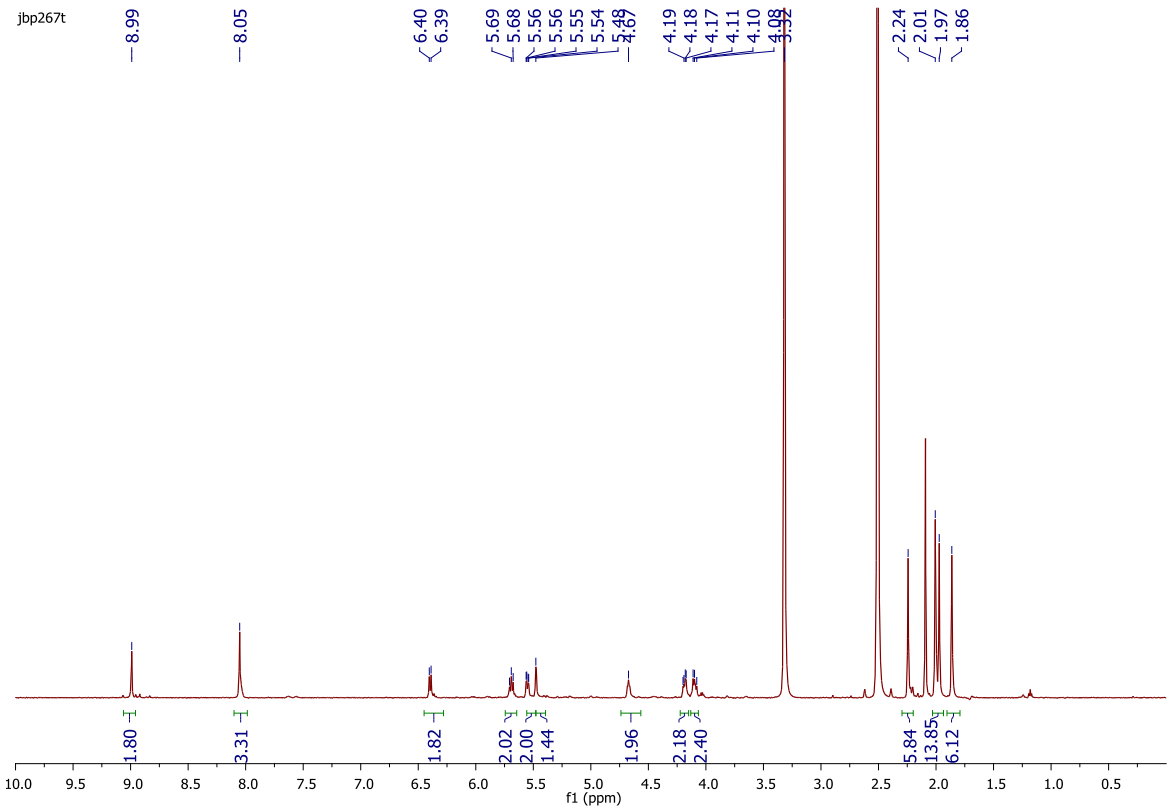

Figure C.8 ^{1}H NMR (600 MHz, DMSO-d_6) spectrum of **98**.

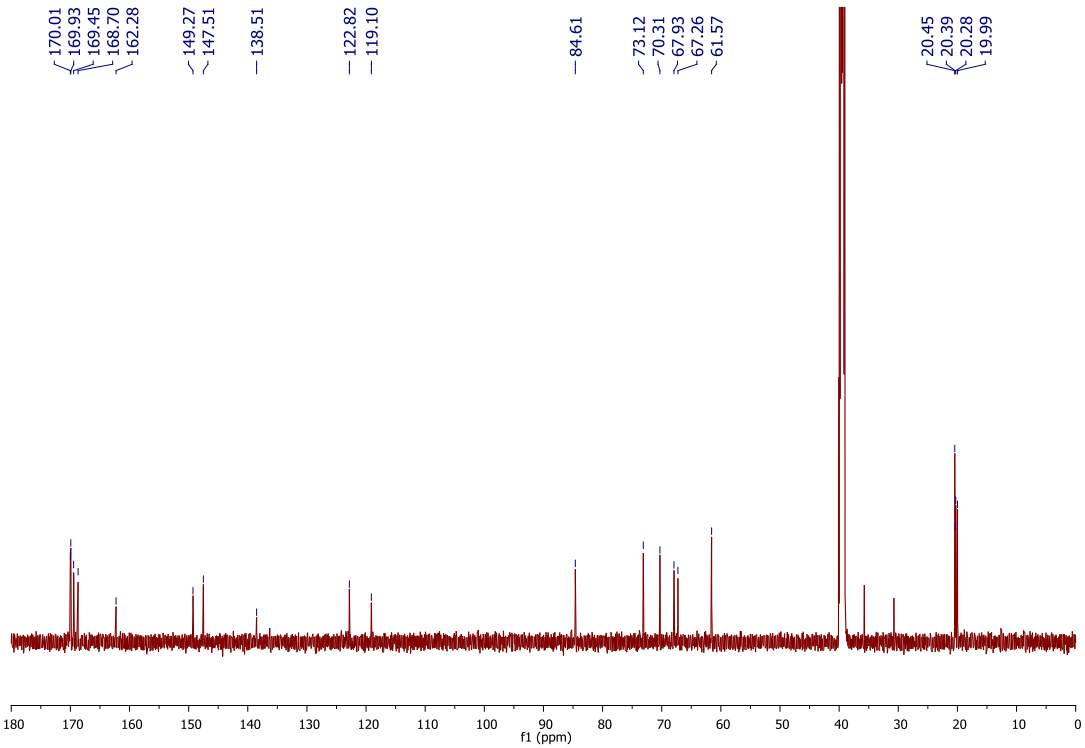

Figure C.9 ^{13}C NMR (150 MHz, DMSO-d_6) spectrum of **98**.

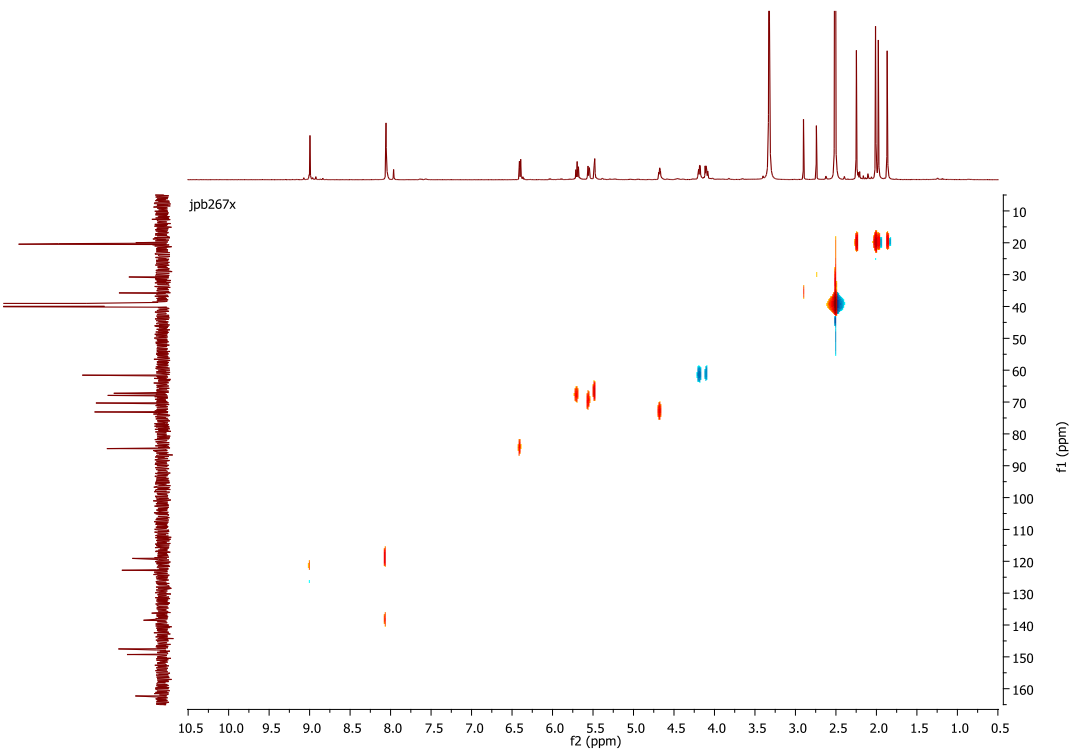

Figure C.10 HSQC of **98**.

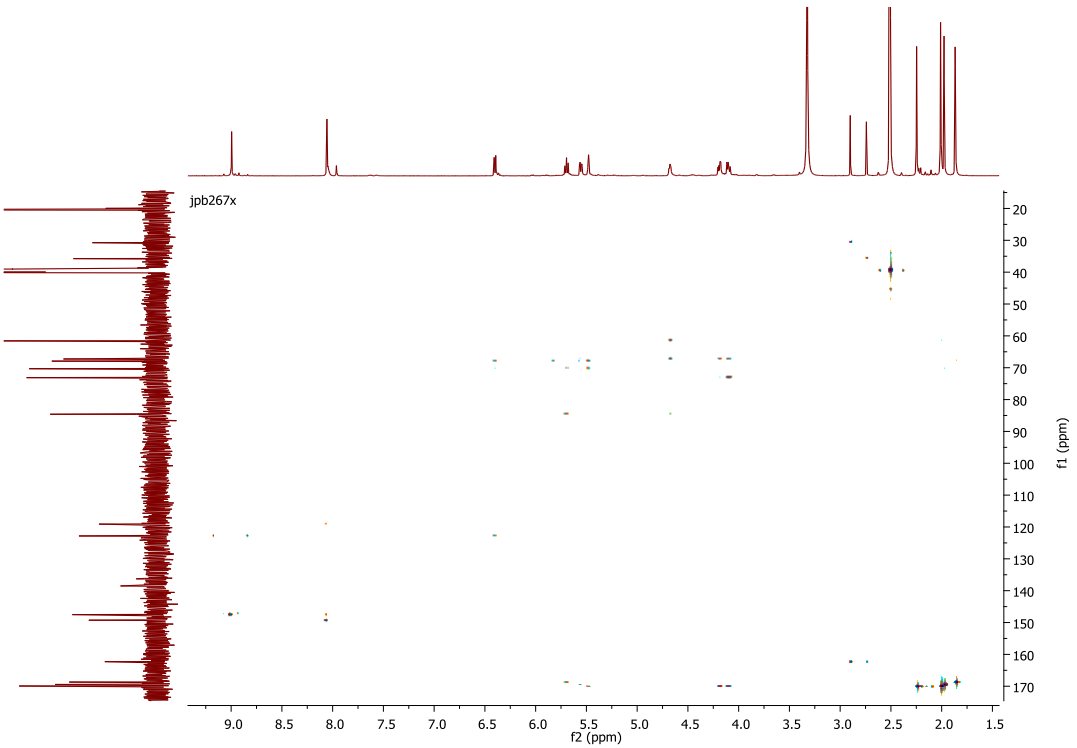

Figure C.11 HMBC of **98**.

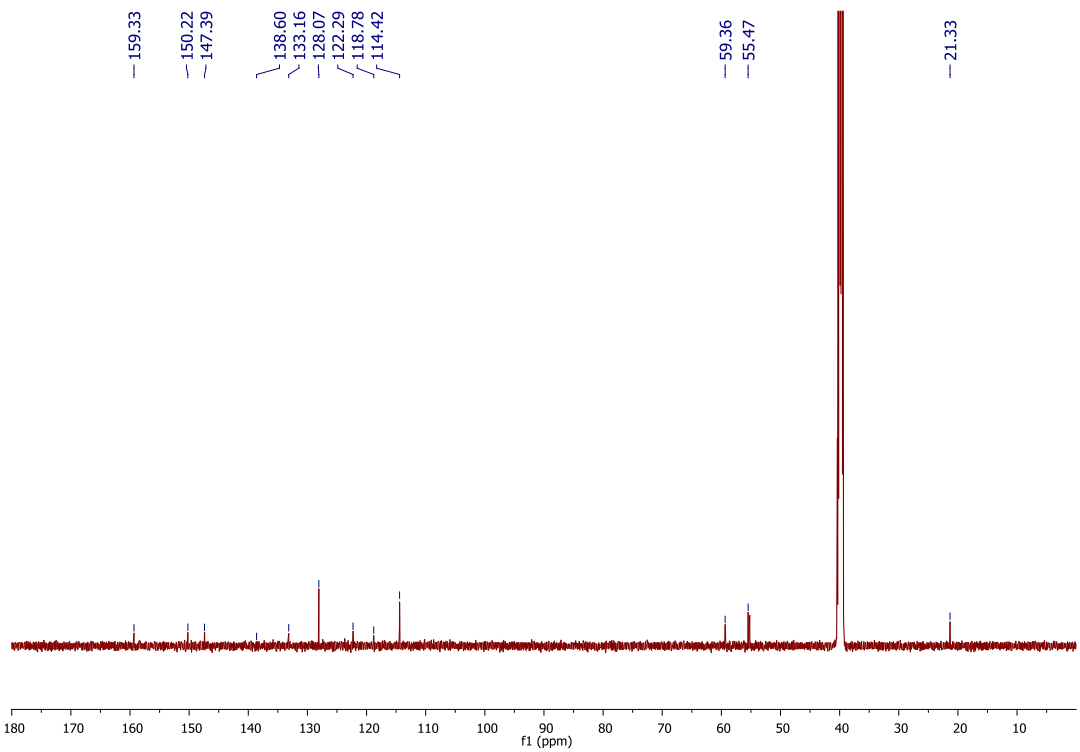

Figure C.12 ^{13}C NMR spectrum (150 MHz, DMSO-d_6) of ligand **99a**.

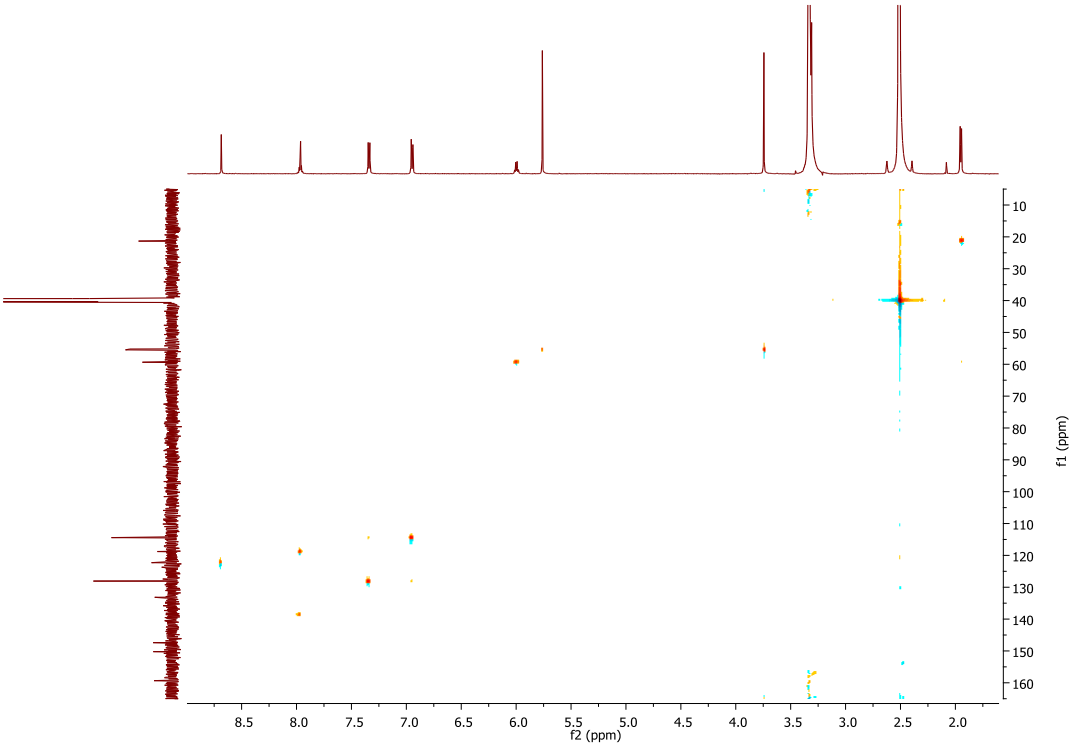

Figure C.13 HSQC of ligand **99a**.

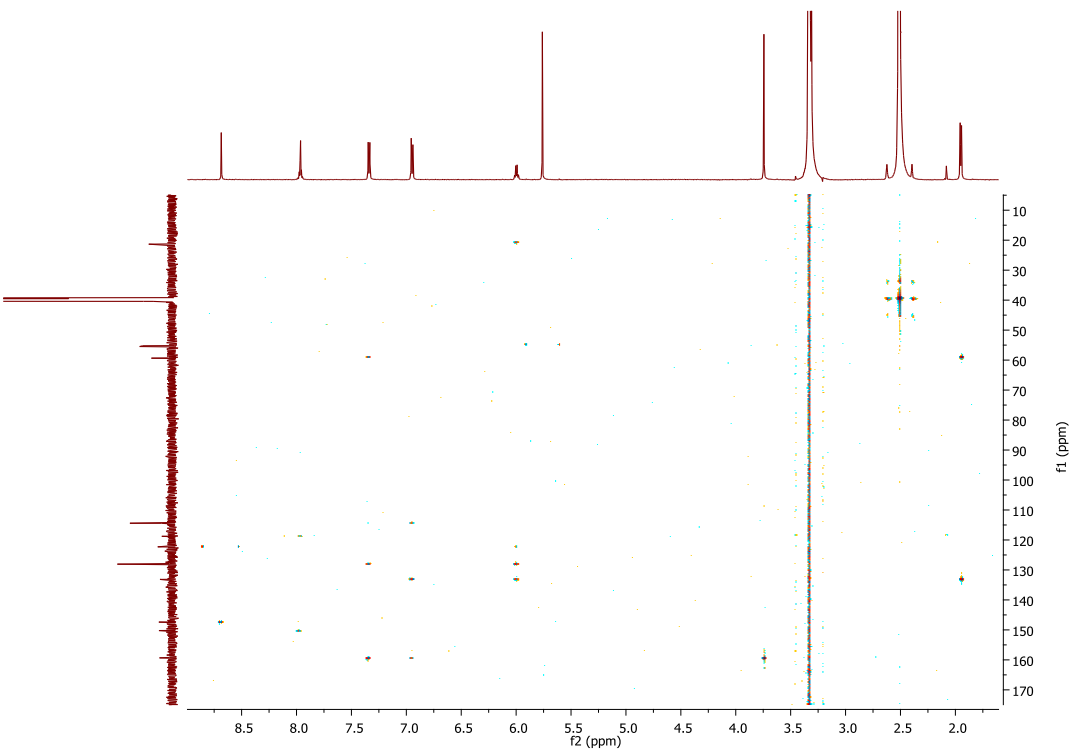

Figure C.14 HMBC of ligand **99a**.

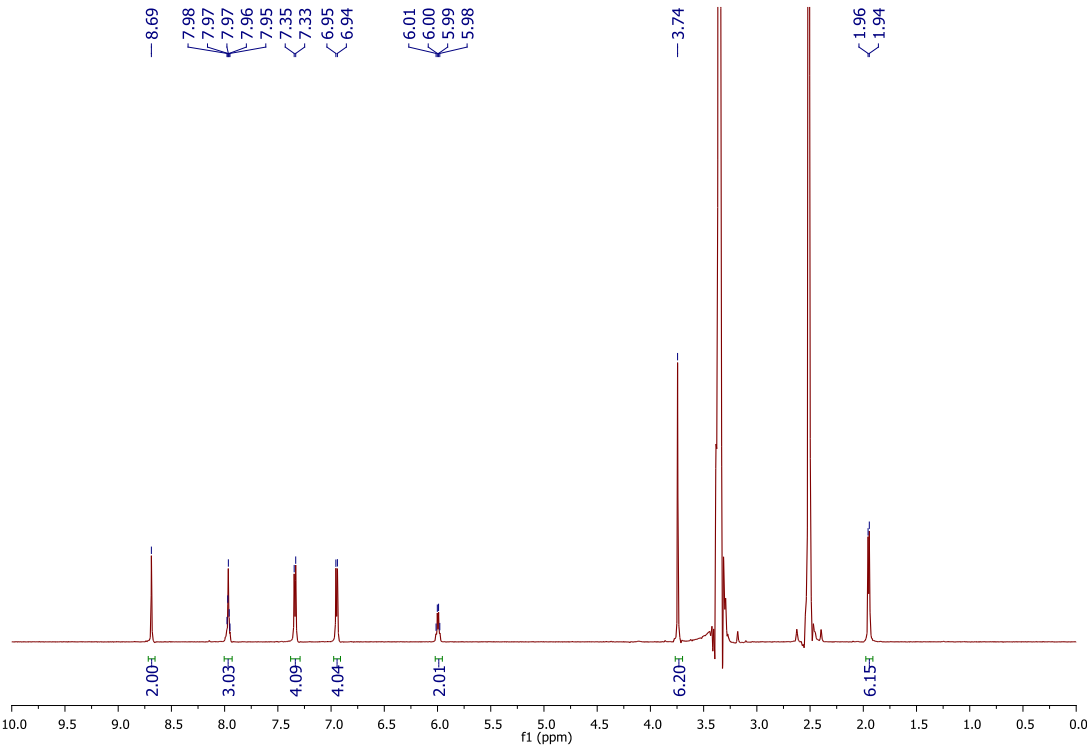

Figure C.15 ^{1}H NMR spectrum (600 MHz, DMSO-d_6) of ligand **99b**.

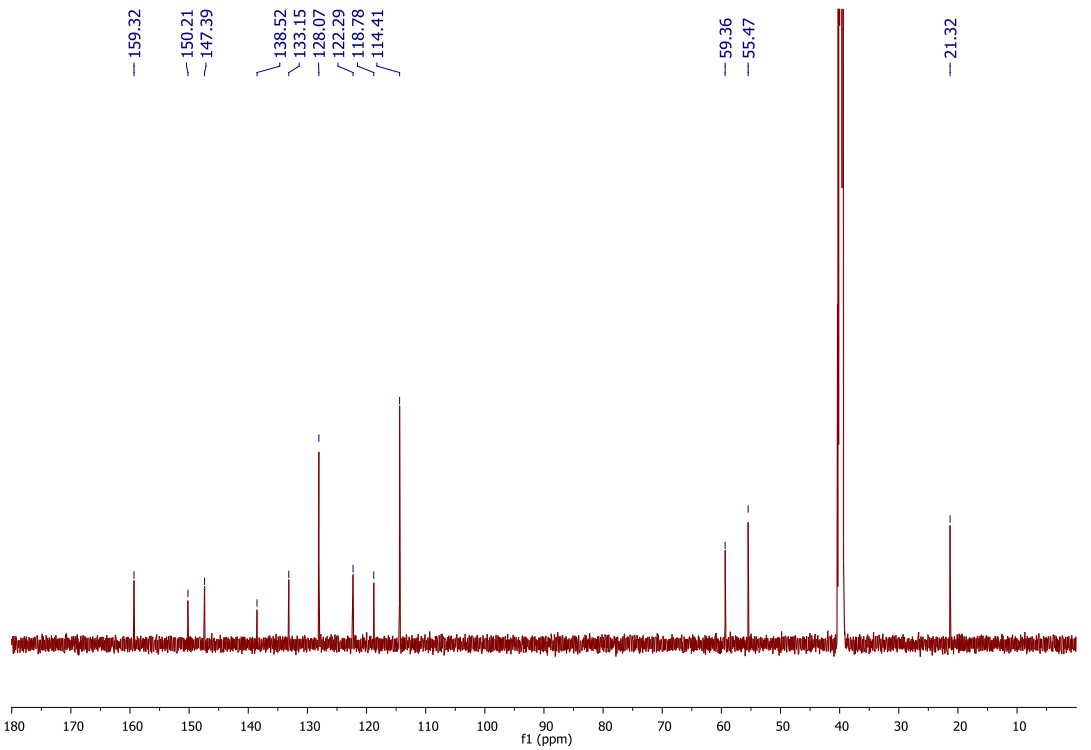

Figure C.16 ^{13}C NMR spectrum (150 MHz, DMSO-d_6) of ligand **99b**.

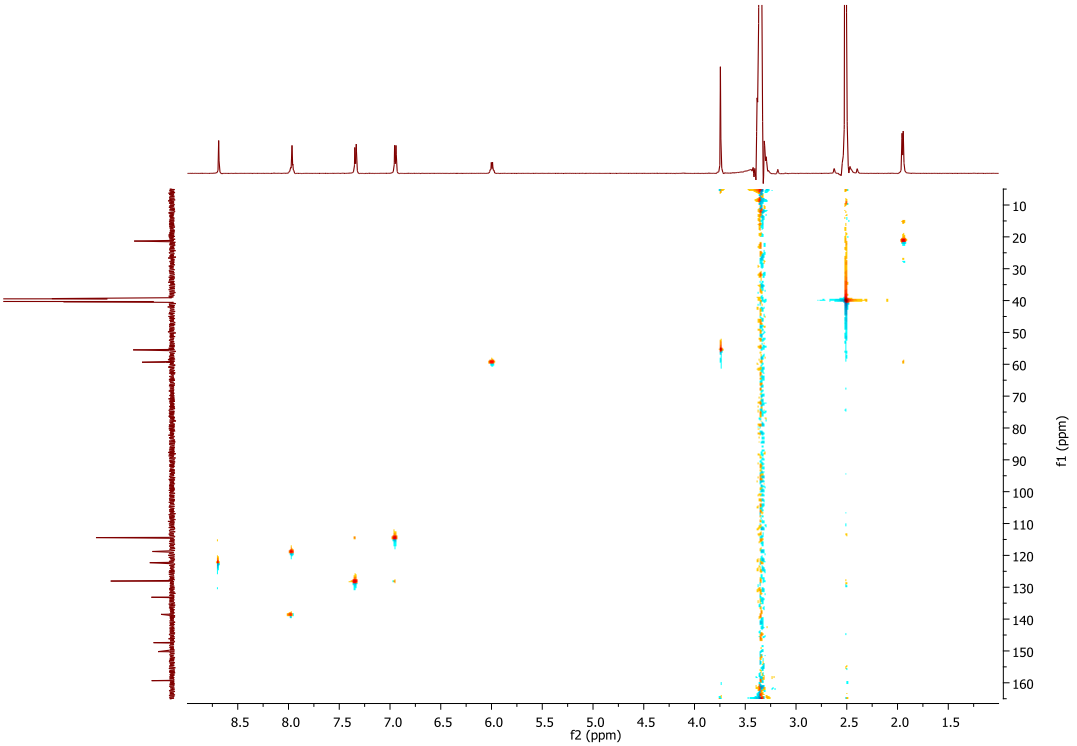

Figure C.17 HSQC of ligand **99b**.

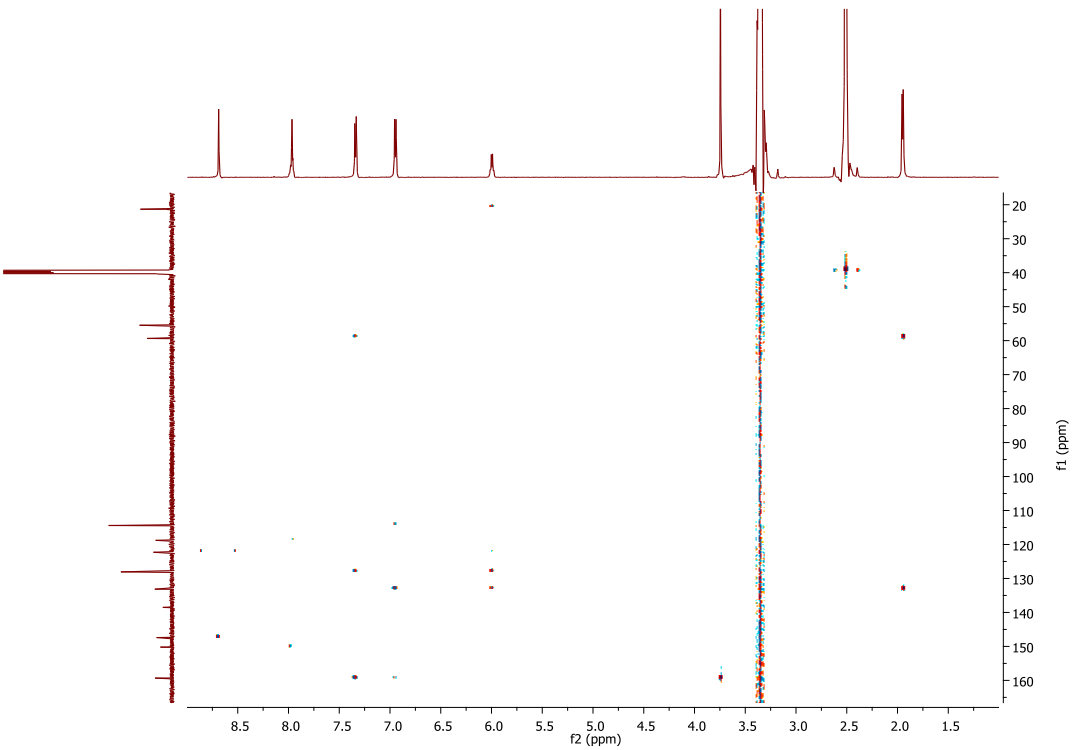

Figure C.18 HMBC of ligand **99b**.

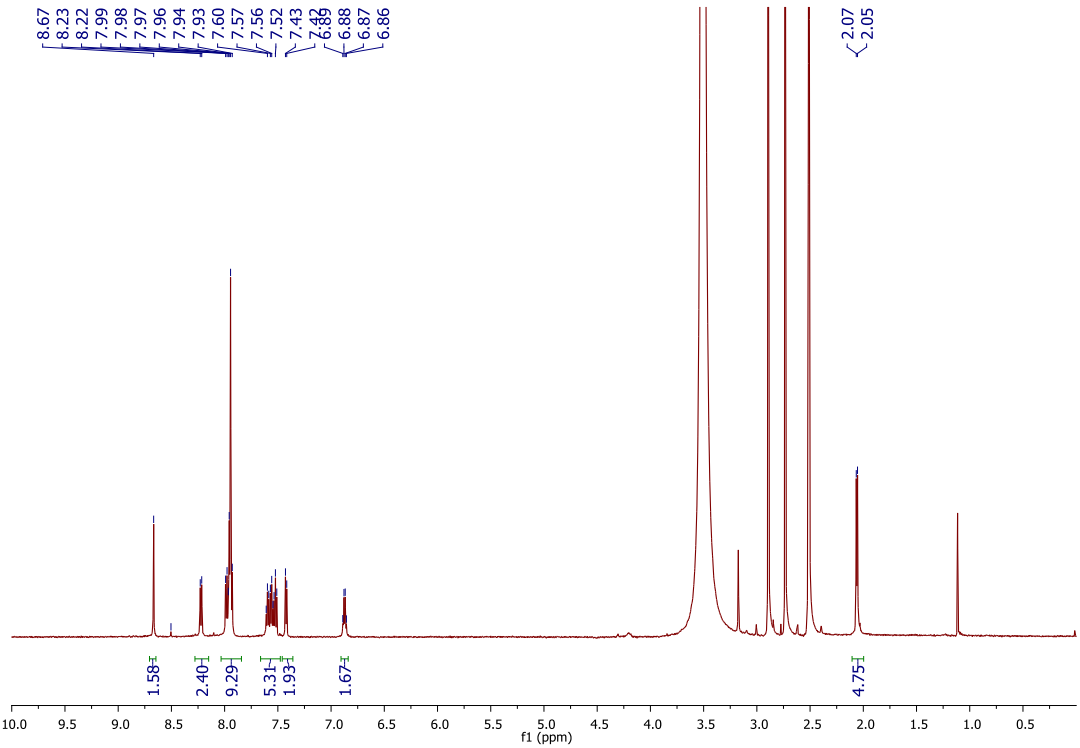

Figure C.19 ^{1}H NMR (600 MHz, DMSO-d_6) spectrum of **100a**.

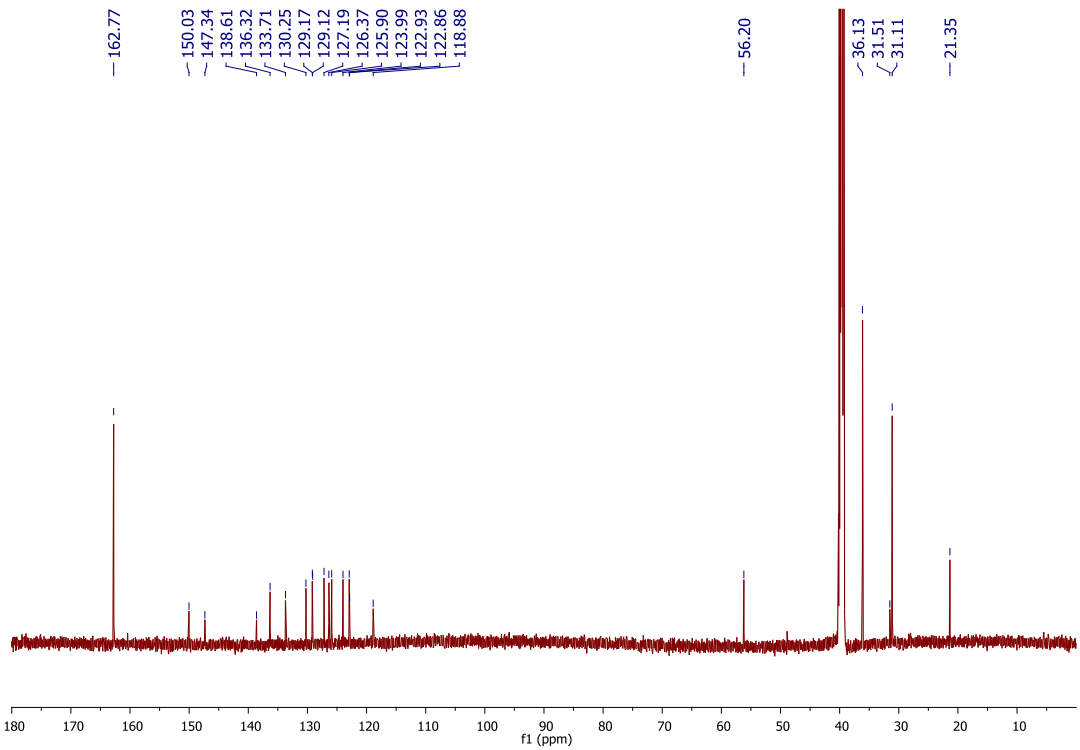

Figure C.20 ^{13}C NMR (150 MHz, DMSO-d_6) spectrum of **100a**.

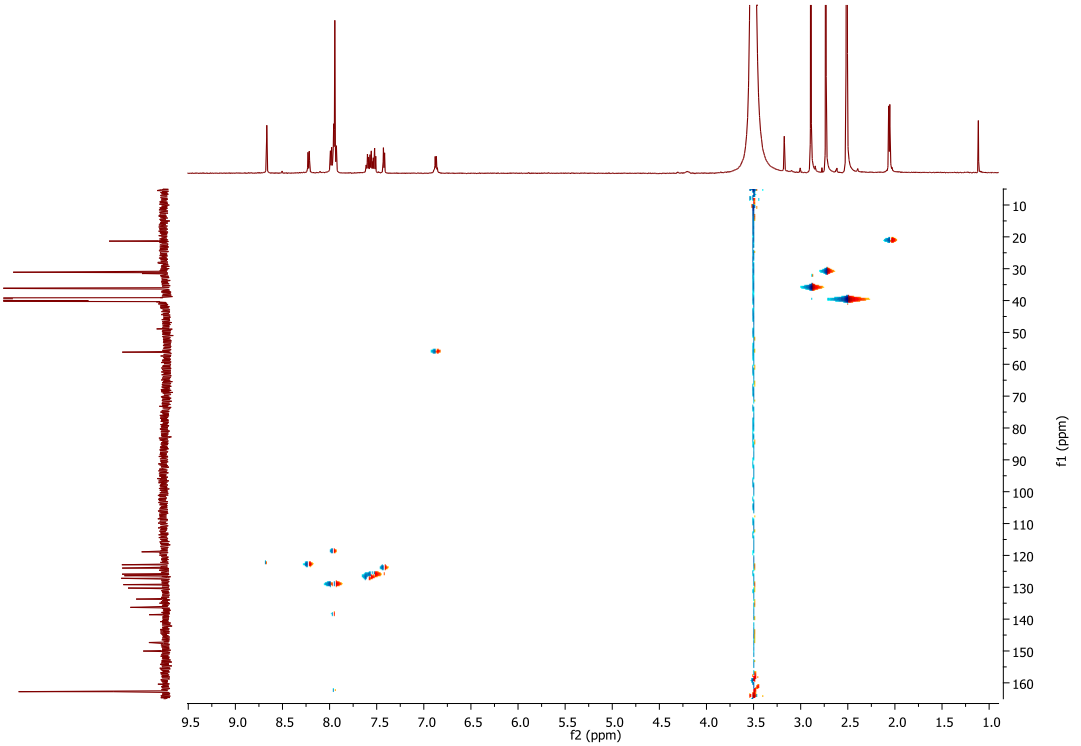

Figure C.21 HSQC of **100a**.

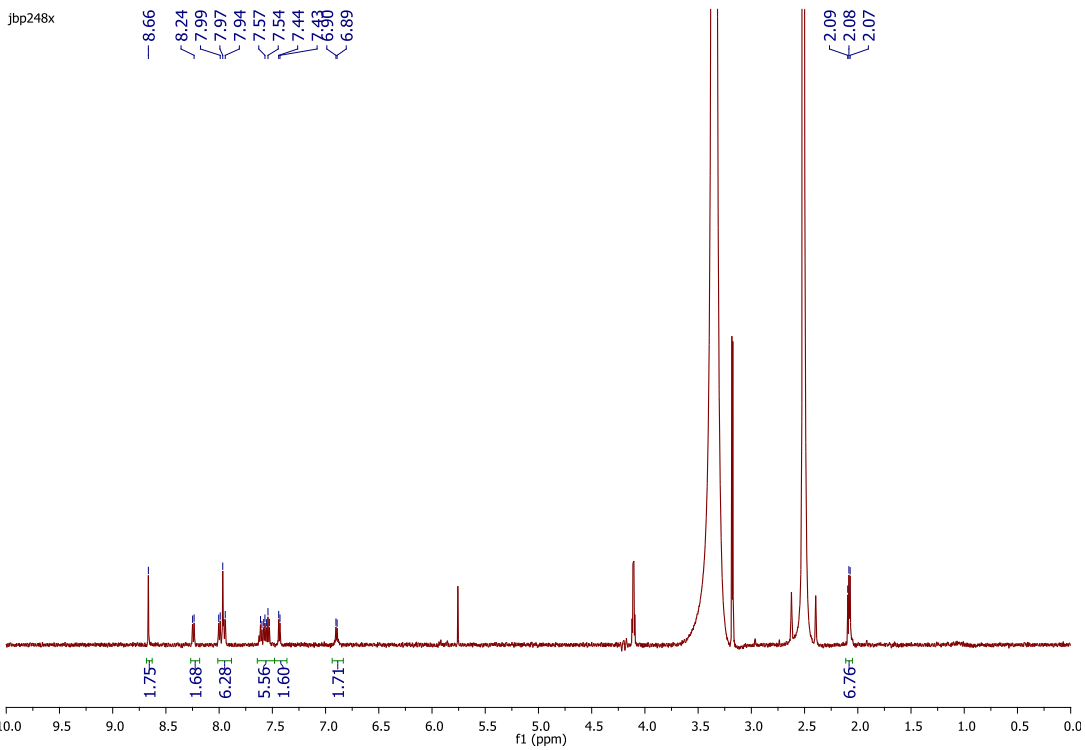

Figure C.22 ^{1}H NMR (600 MHz, DMSO-d_6) spectrum of **100b**.

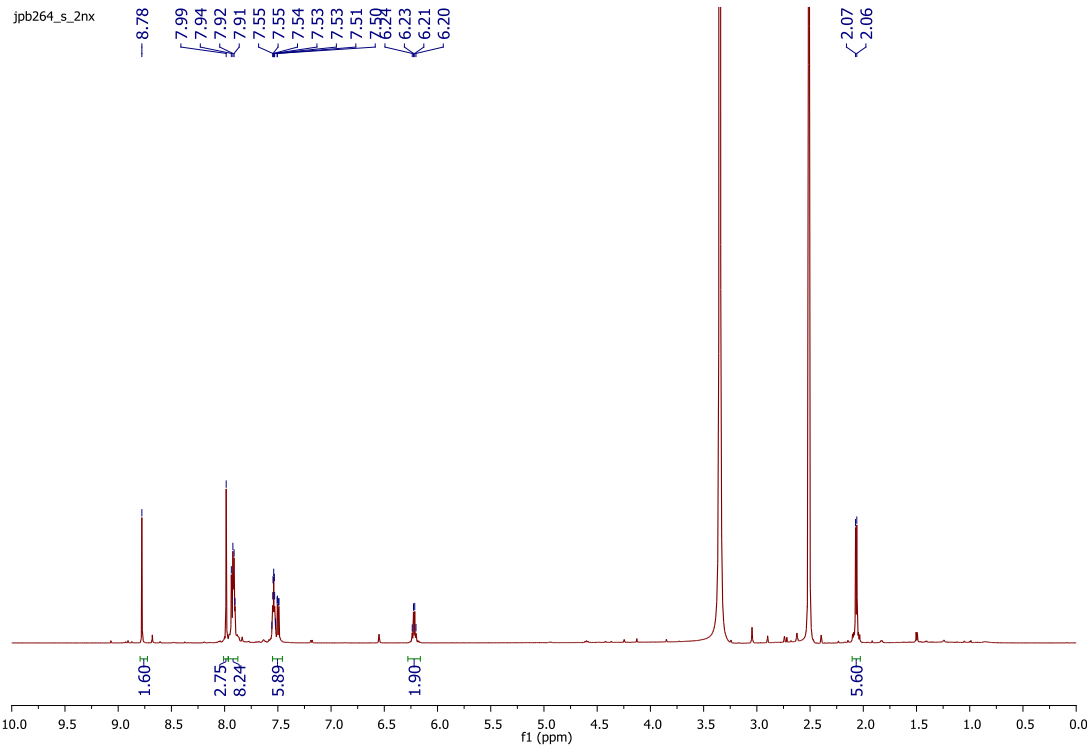

Figure C.23 ^{1}H NMR (600 MHz, DMSO-d_6) spectrum of **101a**.

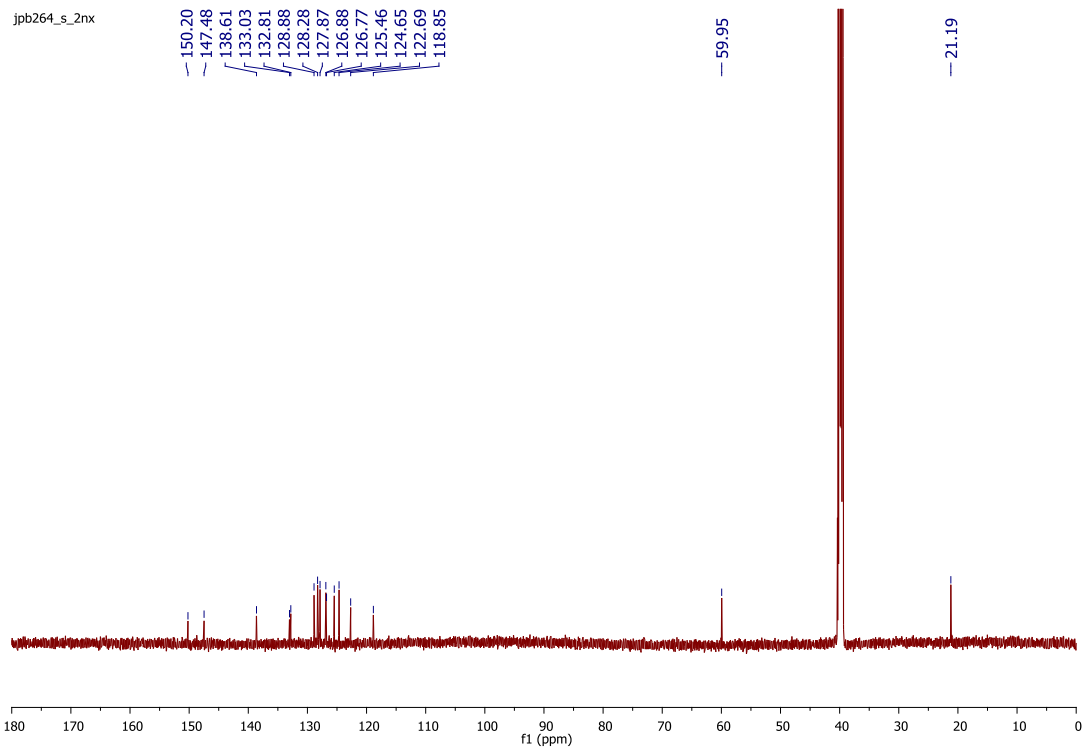

Figure C.24 ^{13}C NMR (150 MHz, DMSO-d_6) spectrum of **101a**.

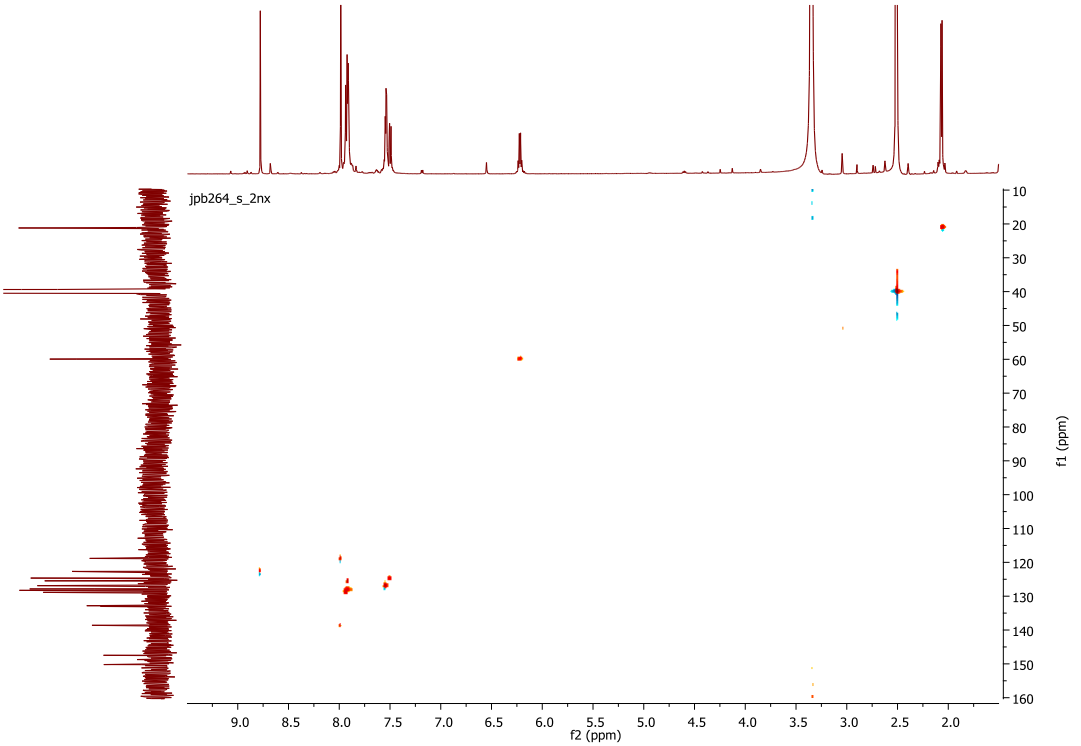

Figure C.25 HSQC of **101a**.

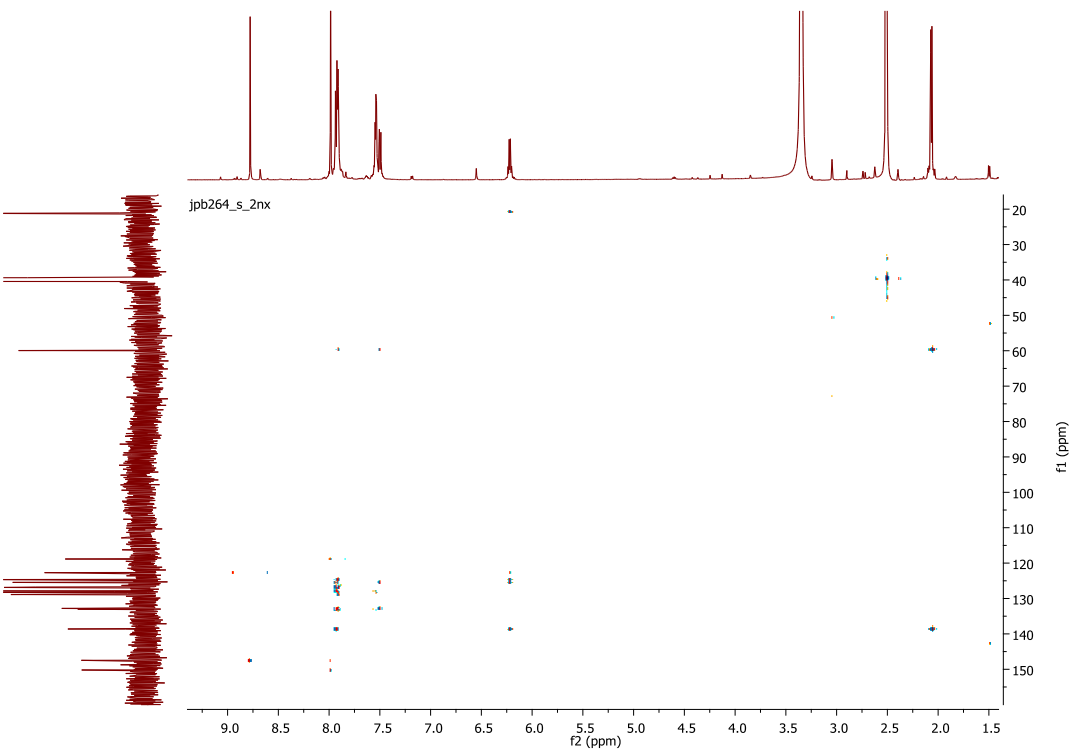

Figure C.26 HMBC of **101a**.

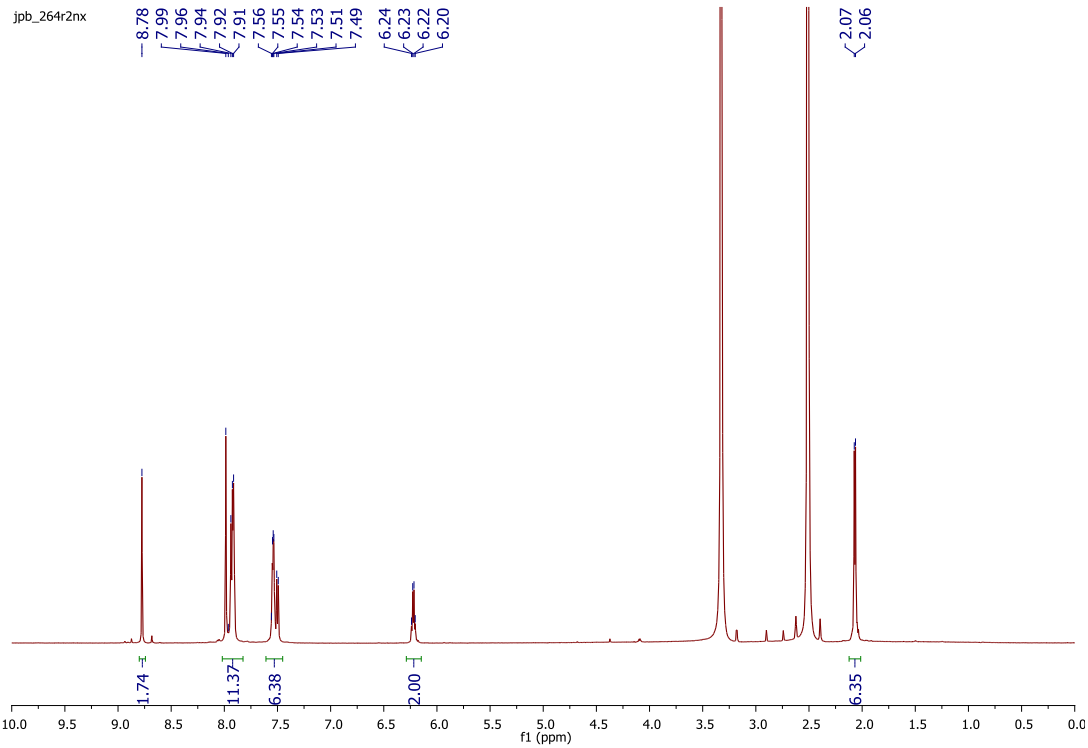

Figure C.27 ^{1}H NMR (600 MHz, DMSO-d_6) spectrum of **101b**.

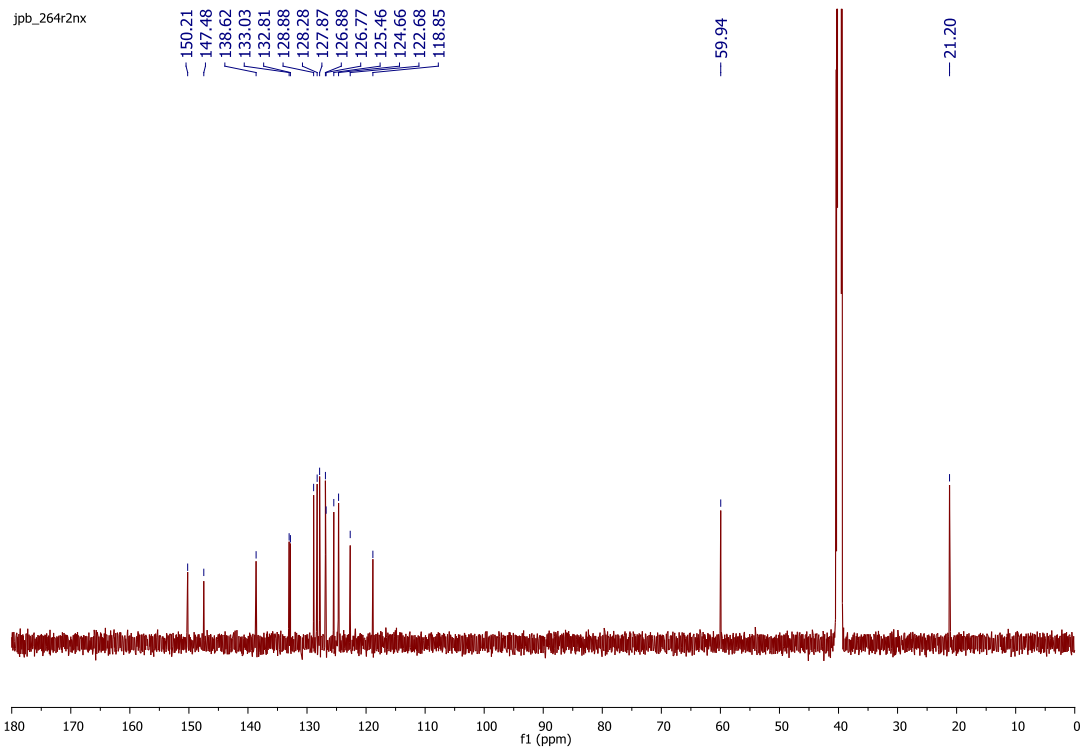

Figure C.28 ^{13}C NMR (150 MHz, DMSO-d_6) spectrum of **101b**.

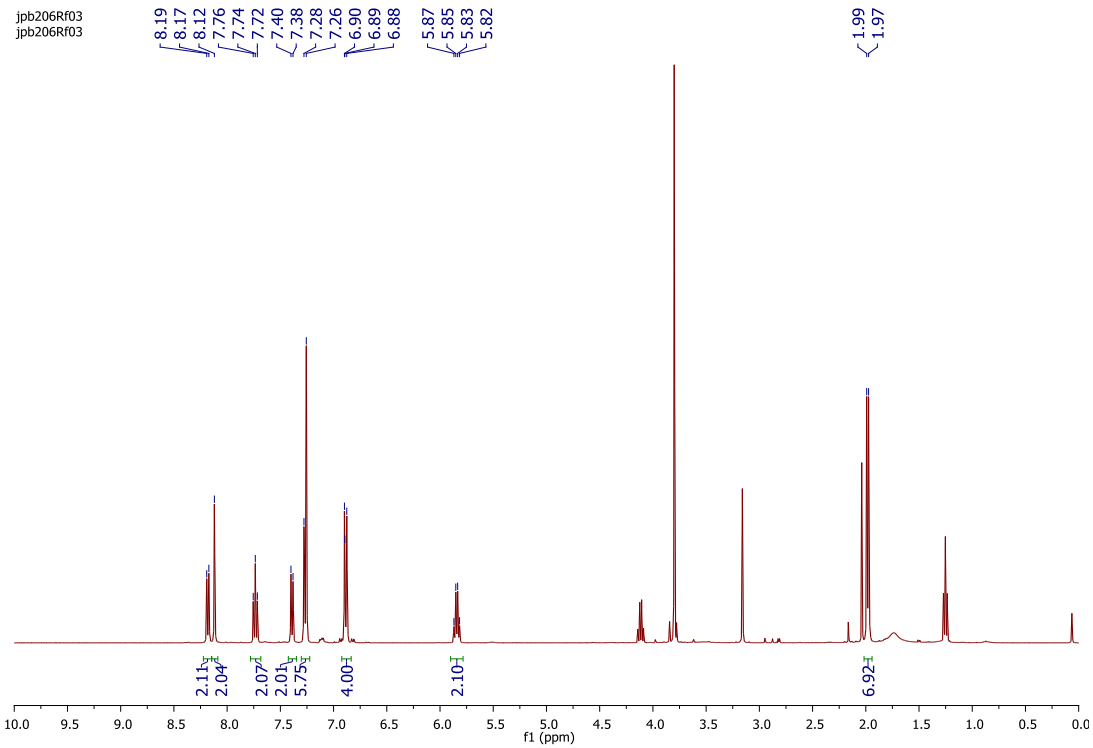

Figure C.29 ^{1}H NMR (400 MHz, $CDCl_3$) of **102**.

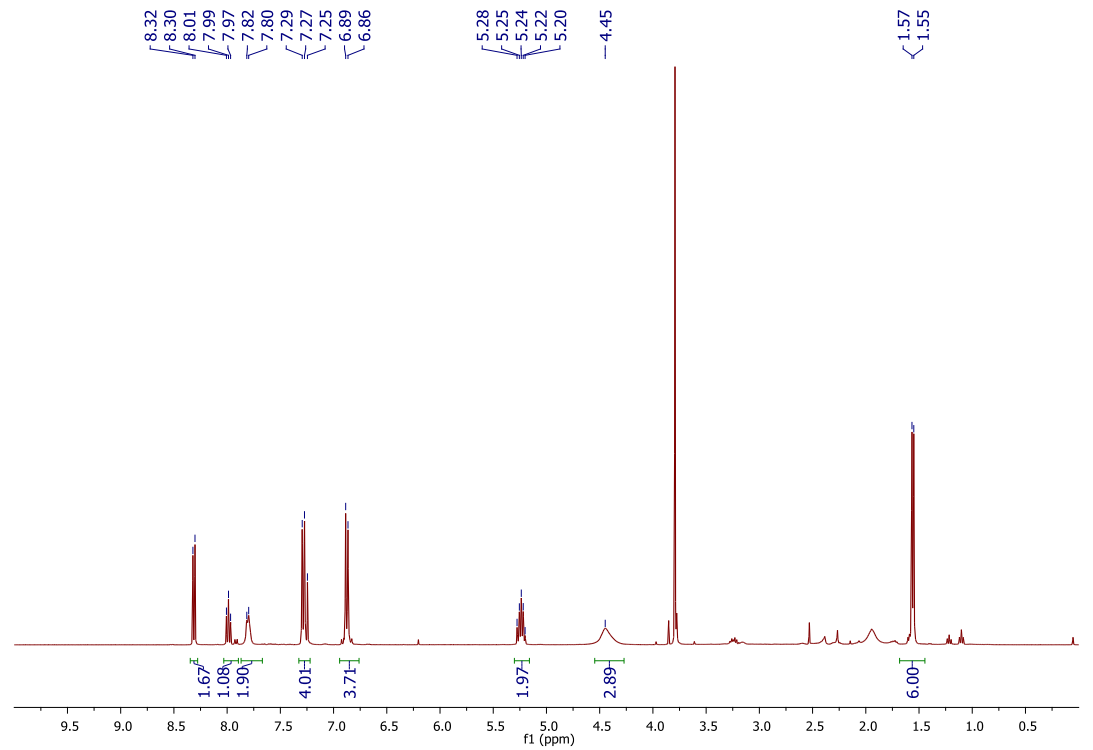

Figure C.30 ^{1}H NMR (400 MHz, $CDCl_3$) of **103**.

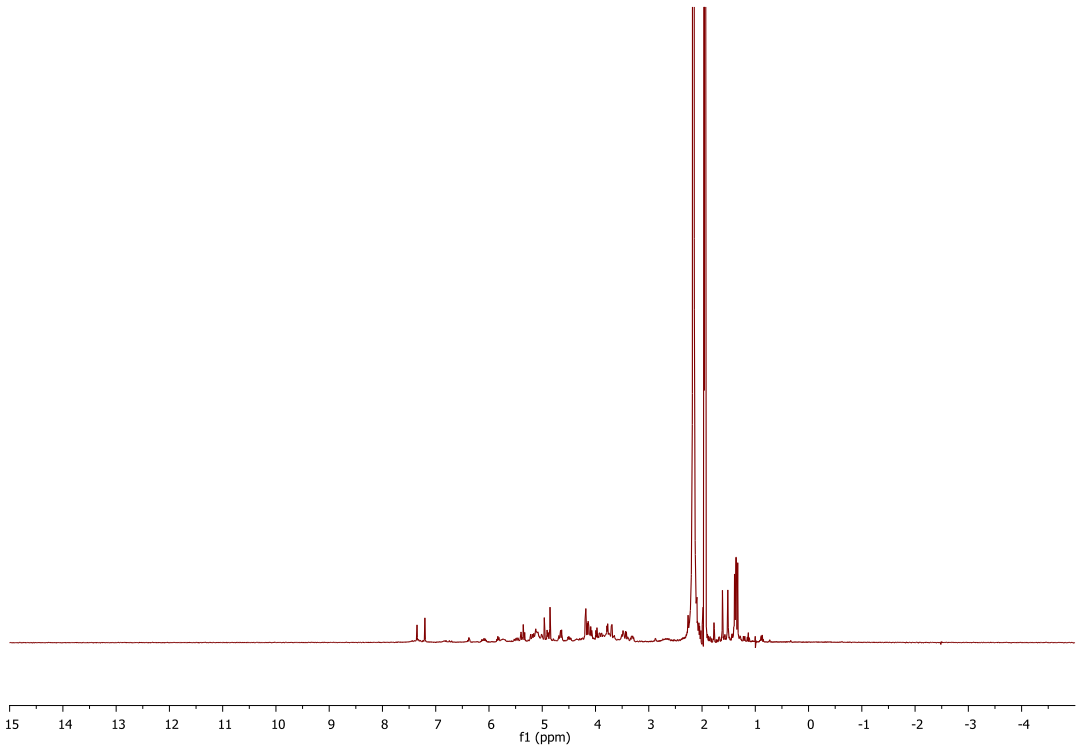

Figure C.31 ^{1}H NMR (400 MHz, CD_3CN) of $[Eu\cdot(\mathbf{96})_3](CF_3SO_3)_3$.

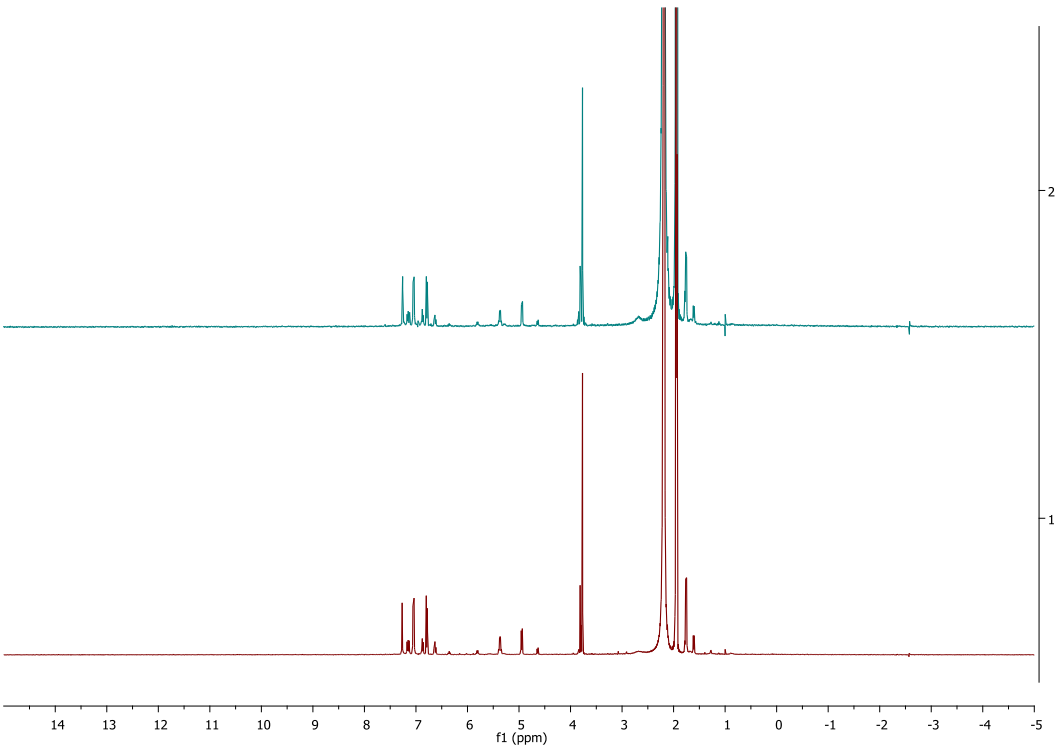

Figure C.32 ^{1}H NMR (400 MHz, CD_3OD) of $[Eu\cdot(\mathbf{99})_3](CF_3SO_3)_3$. (Top: **99a**; Bottom: **99b**.)

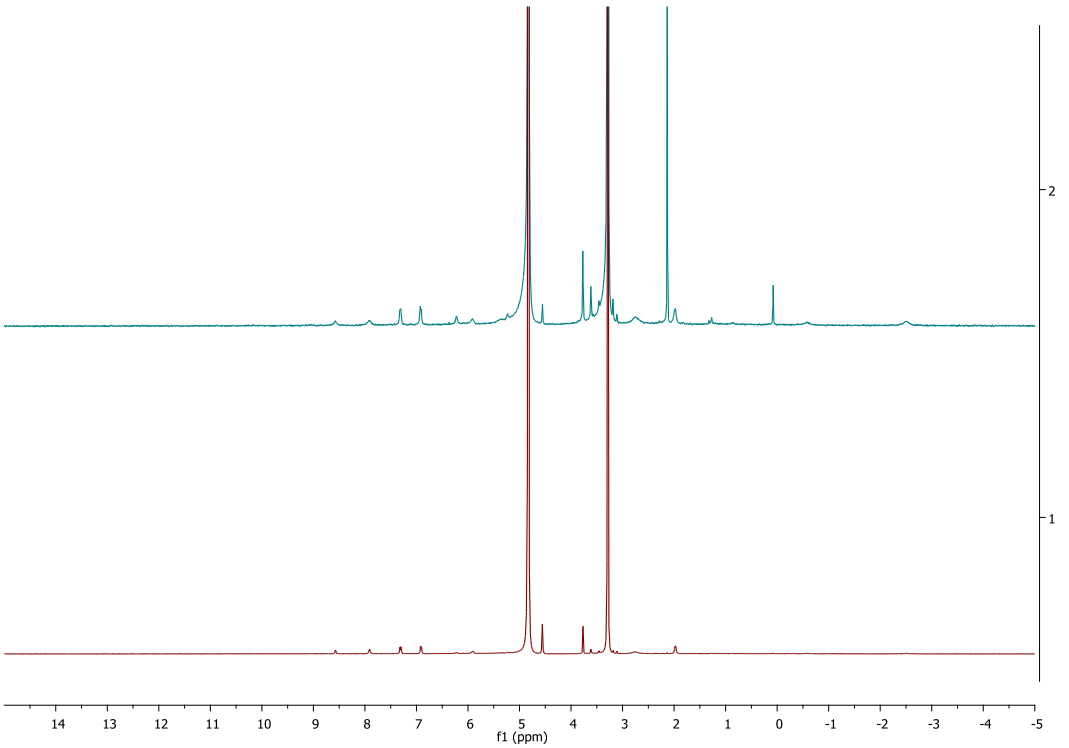

Figure C.33 ^{1}H NMR (400 MHz, CD_3OD) of [Tb·(**99**)$_3$]$(CF_3SO_3)_3$. (Top: **99a**; Bottom: **99b**.)

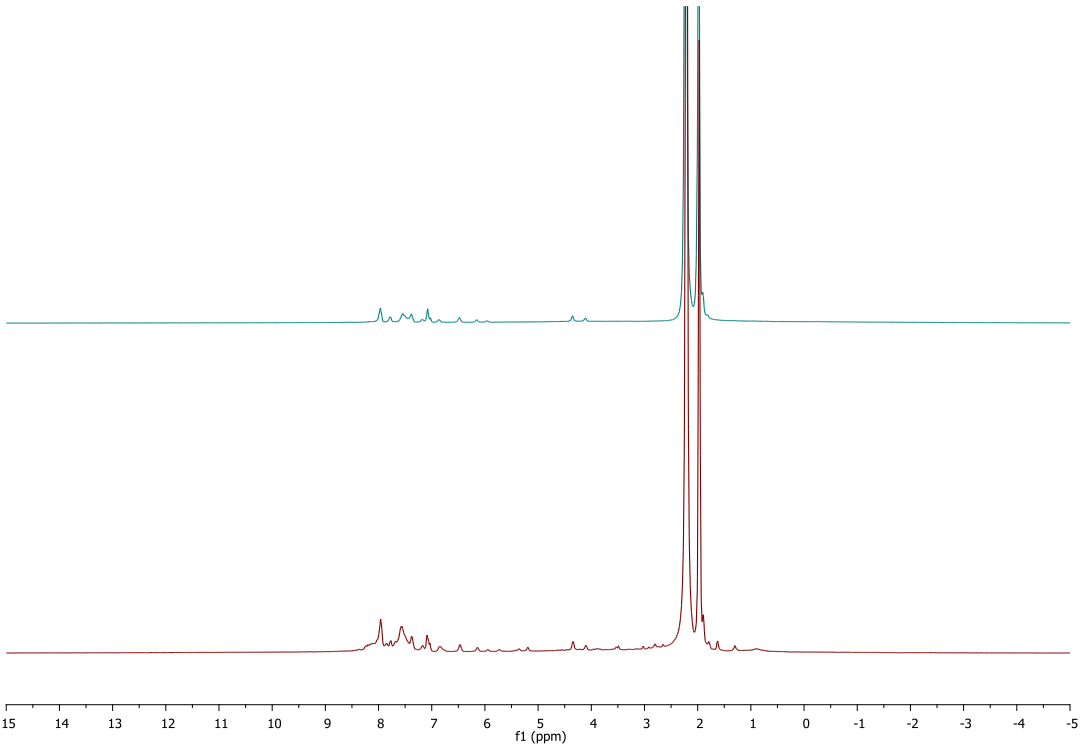

Figure C.34 ^{1}H NMR (400 MHz, CD_3CN) of [Eu·(**100**)$_3$]$(CF_3SO_3)_3$. (Top: **100a**; Bottom: **100b**.)

C.2. Infrared spectra

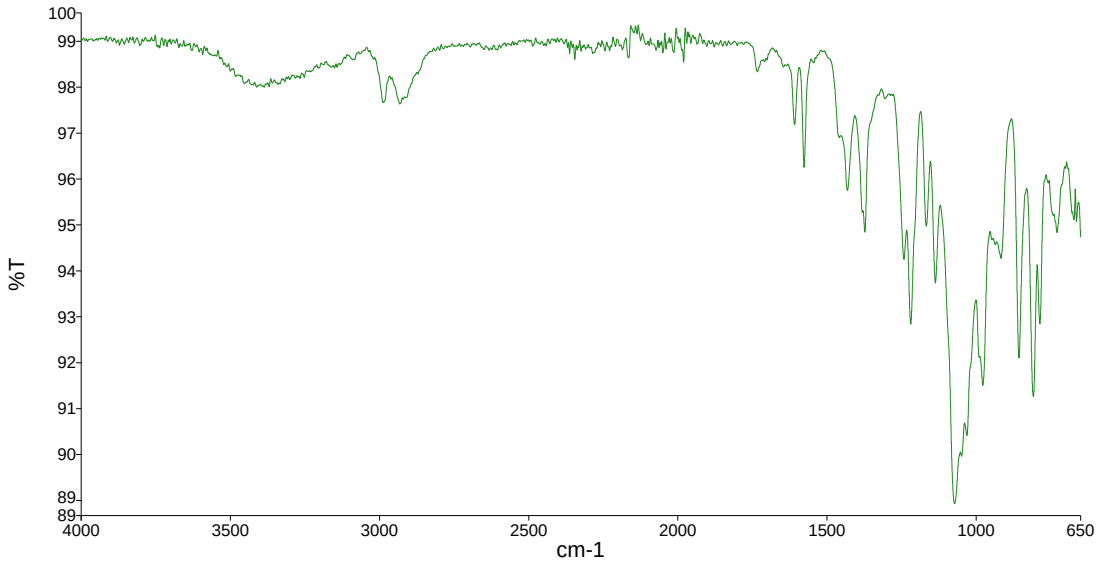

Figure C.35 IR spectrum of ligand **96**.

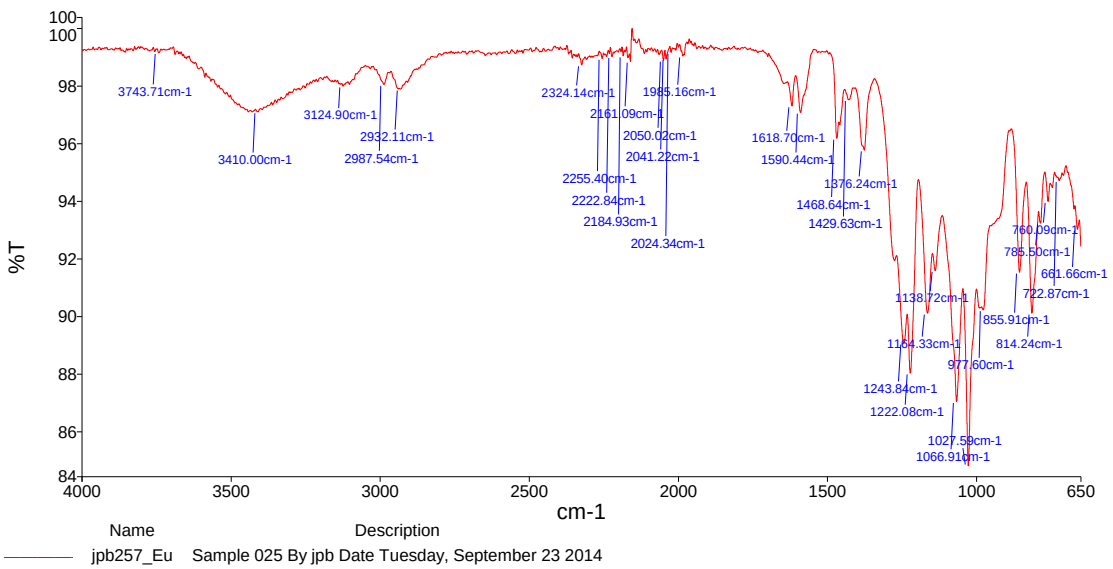

Figure C.36 IR spectrum of ligand $[Eu\cdot(\mathbf{96})_3](CF_3SO_3)_3$.

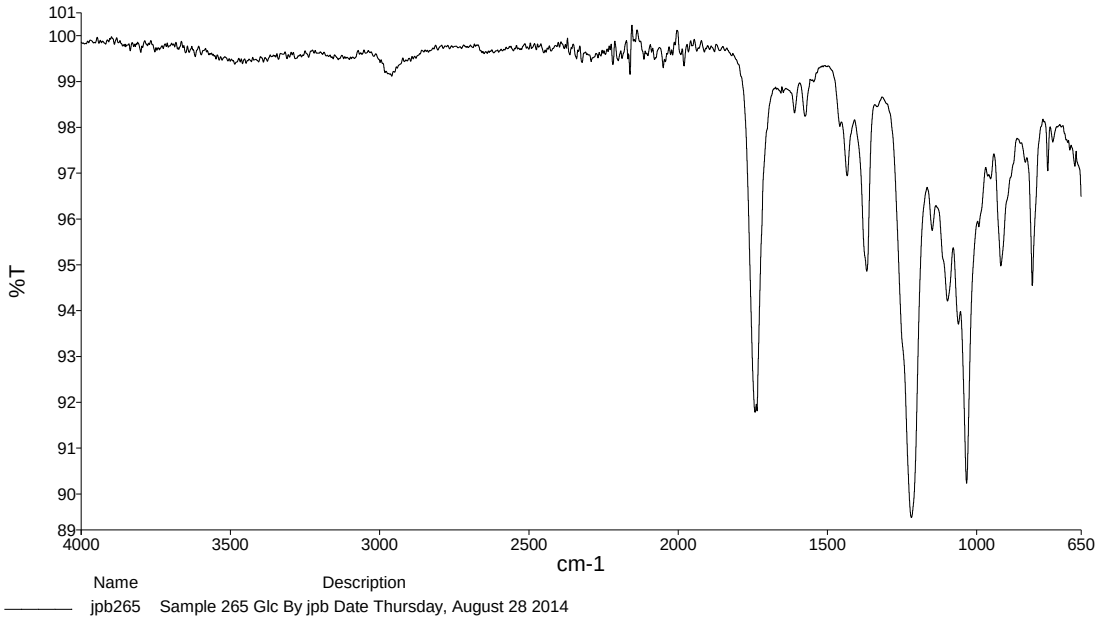

Figure C.37 IR spectrum of ligand **97**.

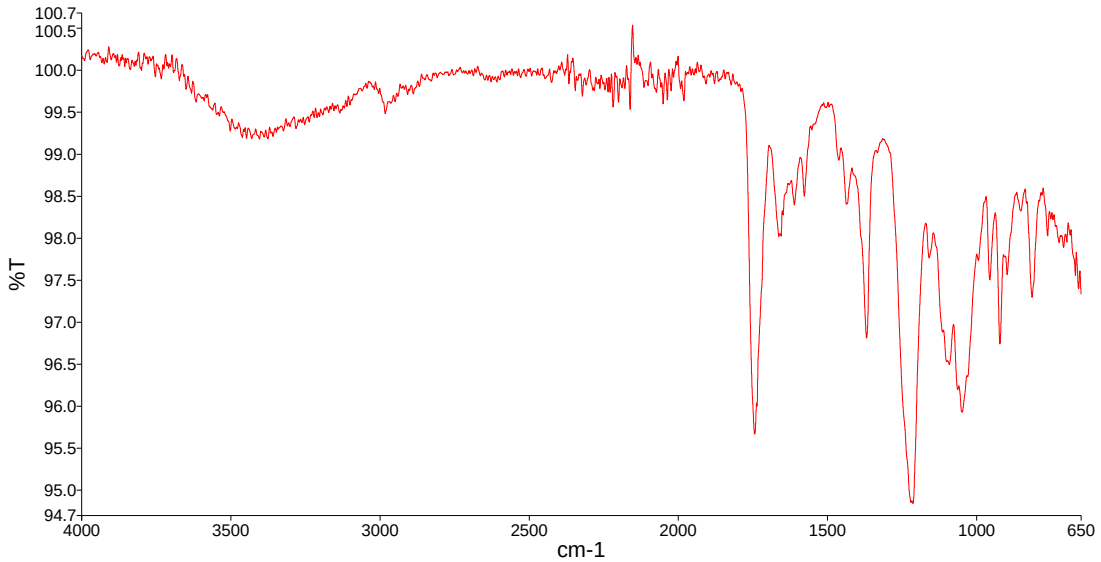

Figure C.38 IR spectrum of ligand **98**.

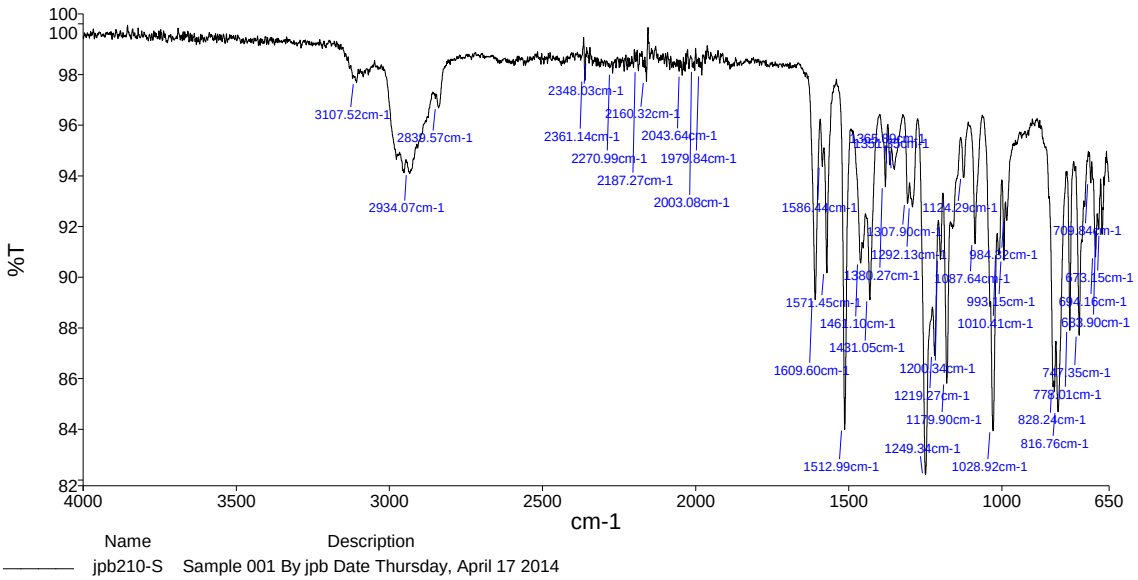

Figure C.39 IR spectrum of ligand **99a**.

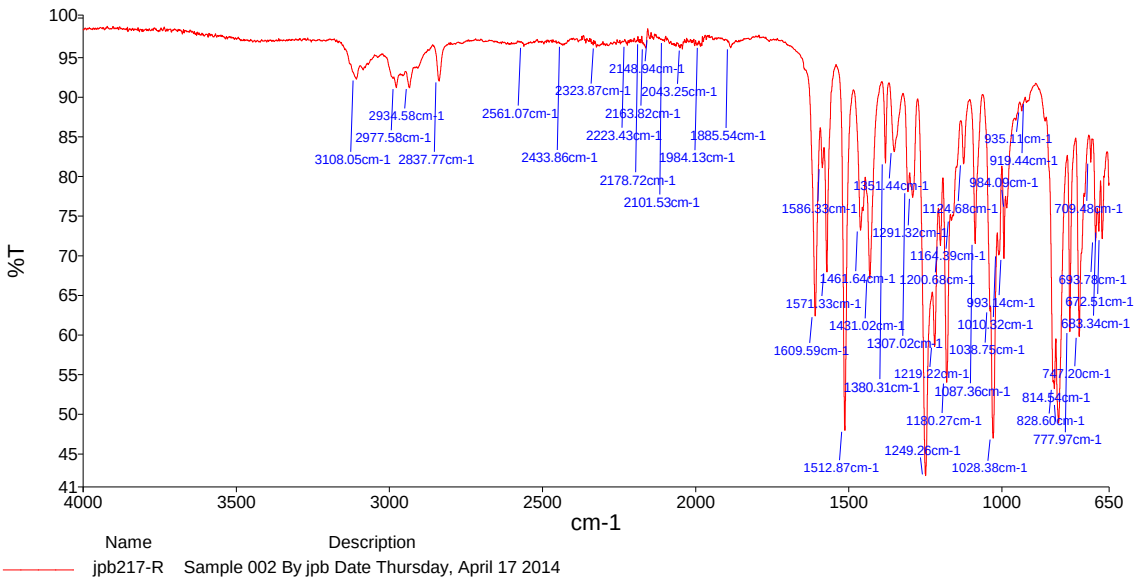

Figure C.40 IR spectrum of ligand **99b**.

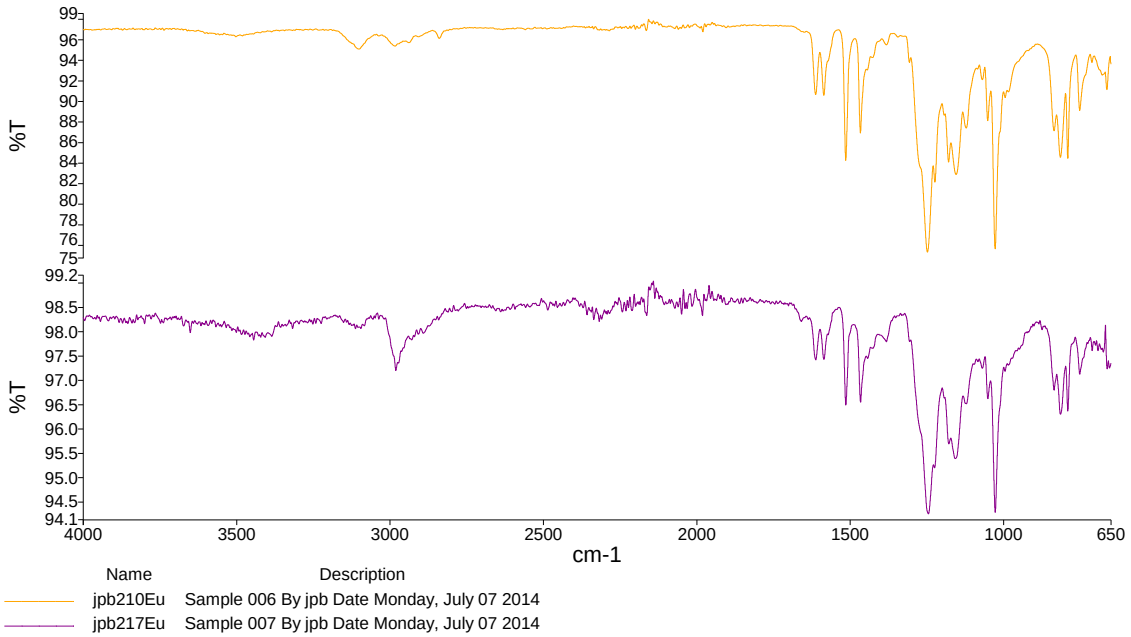

Figure C. 41 IR spectra of Eu(III) complexes of ligands **99a** and **99b**.

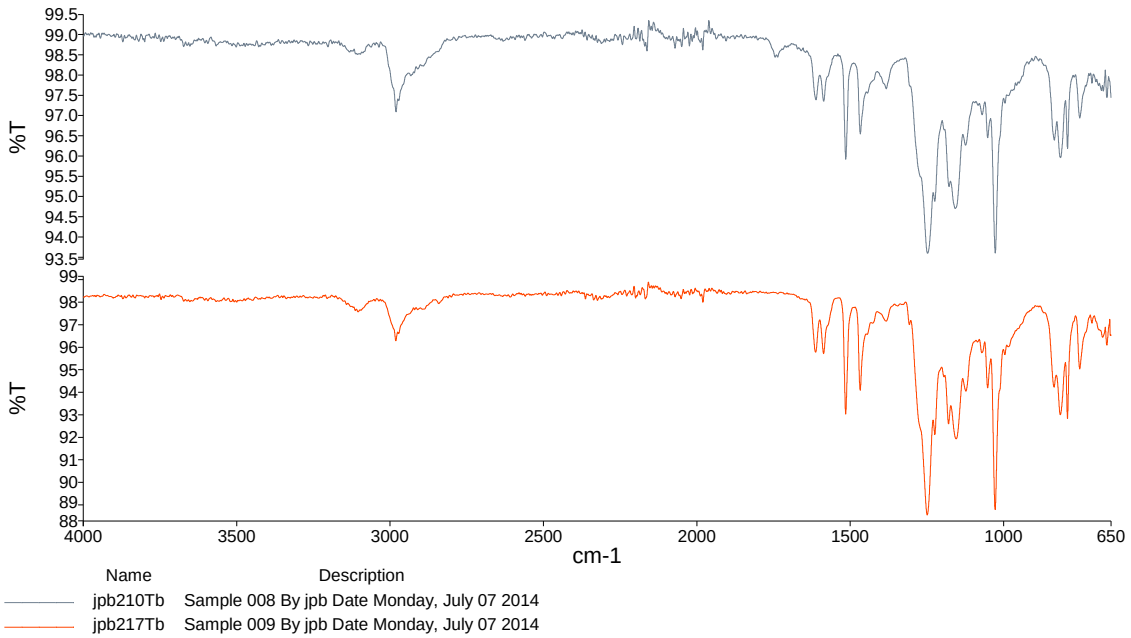

Figure C. 42 IR spectra of Tb(III) complexes of ligands **99a** and **99b**.

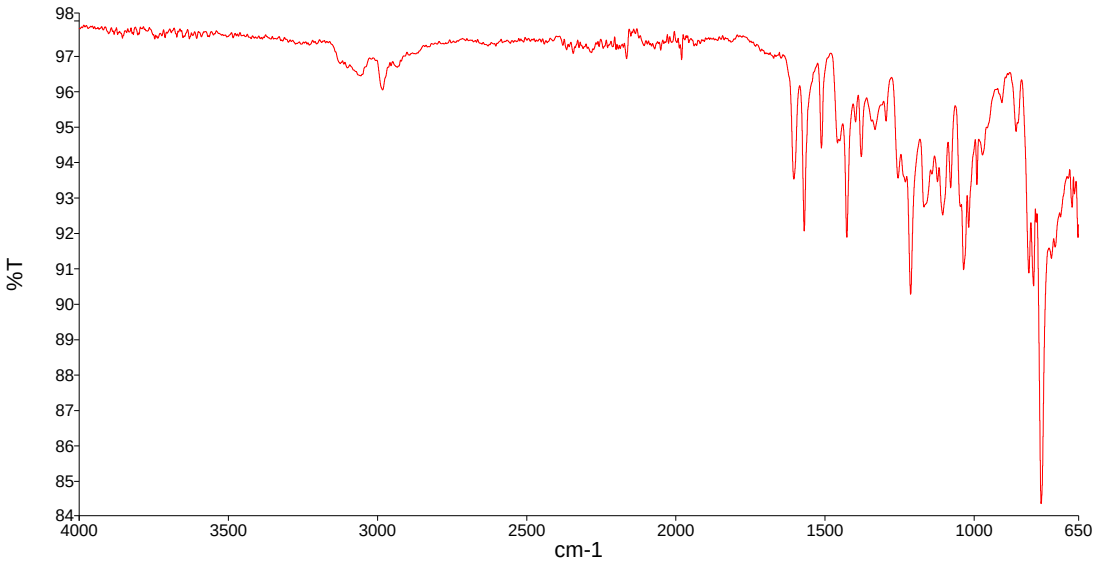

Figure C.43 IR spectrum of ligand **100a**.

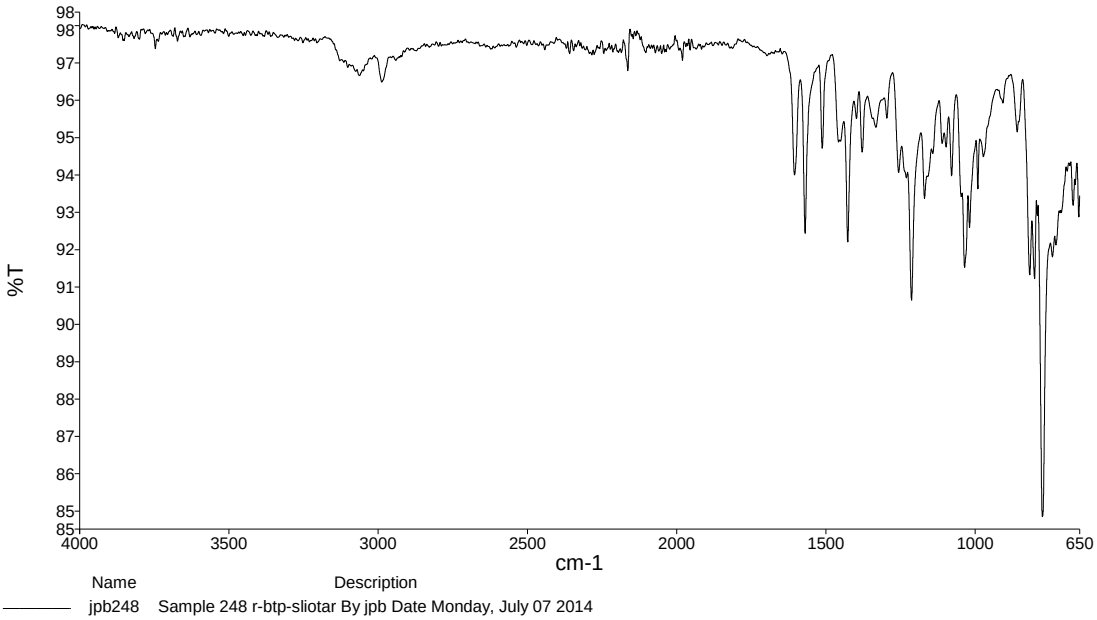

Figure C.44 IR spectrum of ligand **100b**.

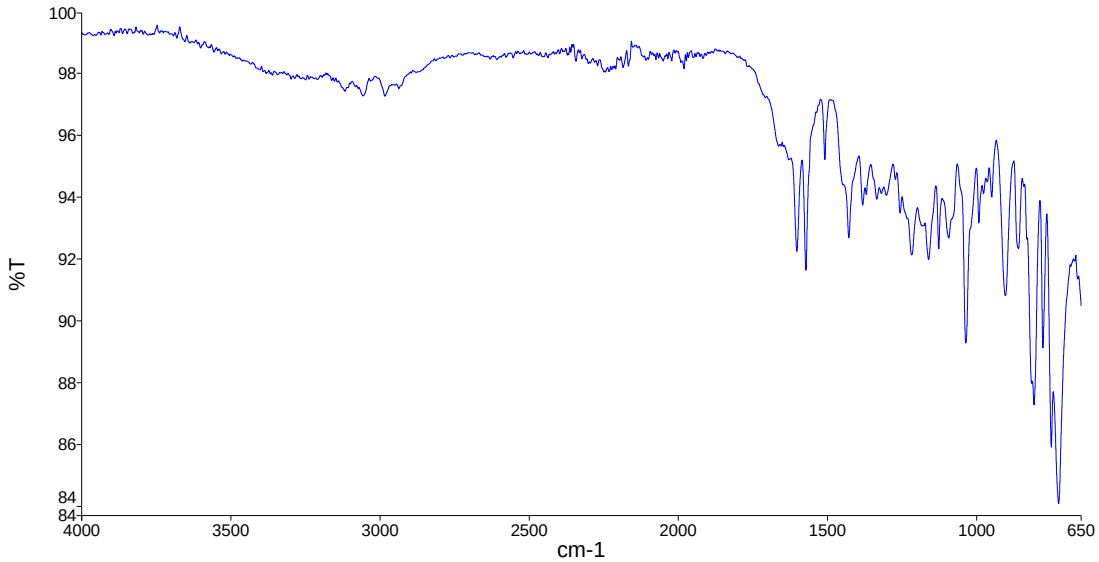

Figure C.45 IR spectrum of **101a**.

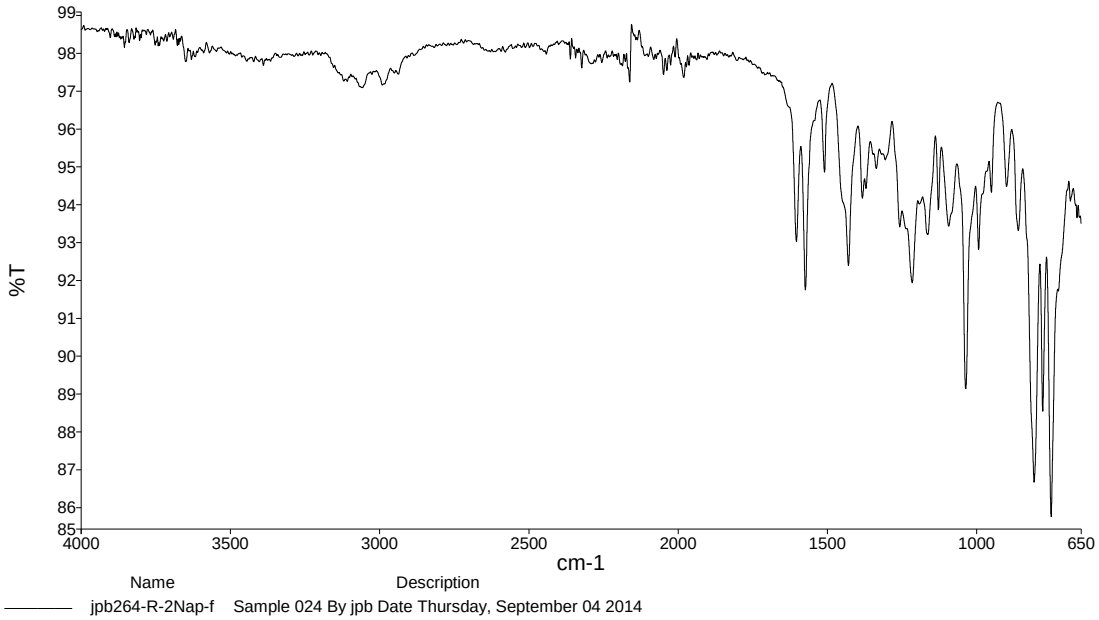

Figure C.46 IR spectrum of ligand **101b**.

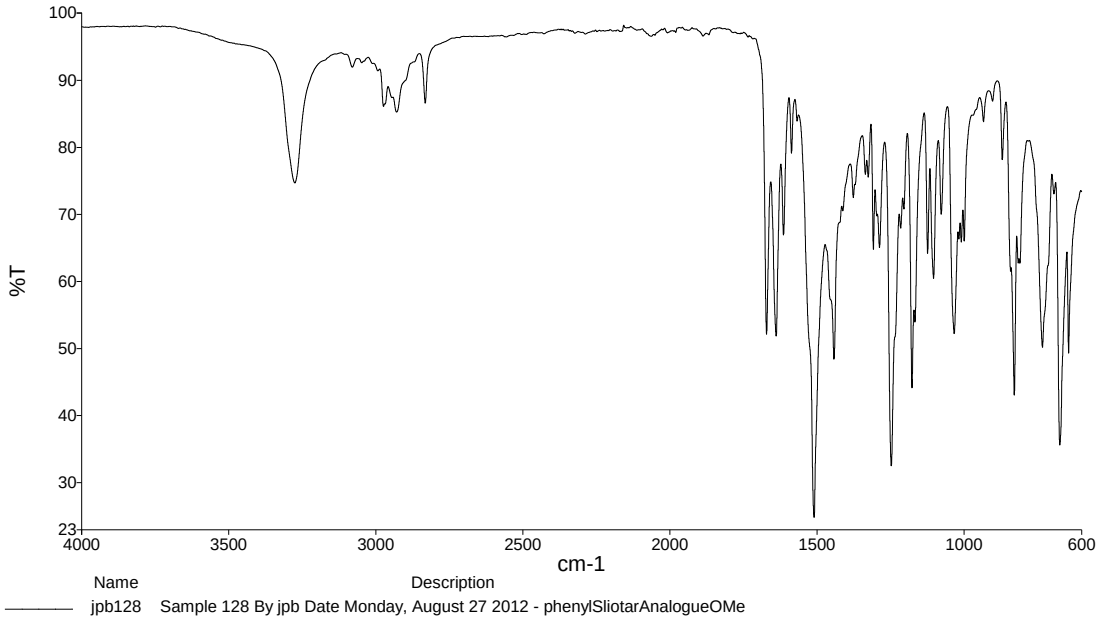

Figure C.47 IR spectrum of ligand **103**.

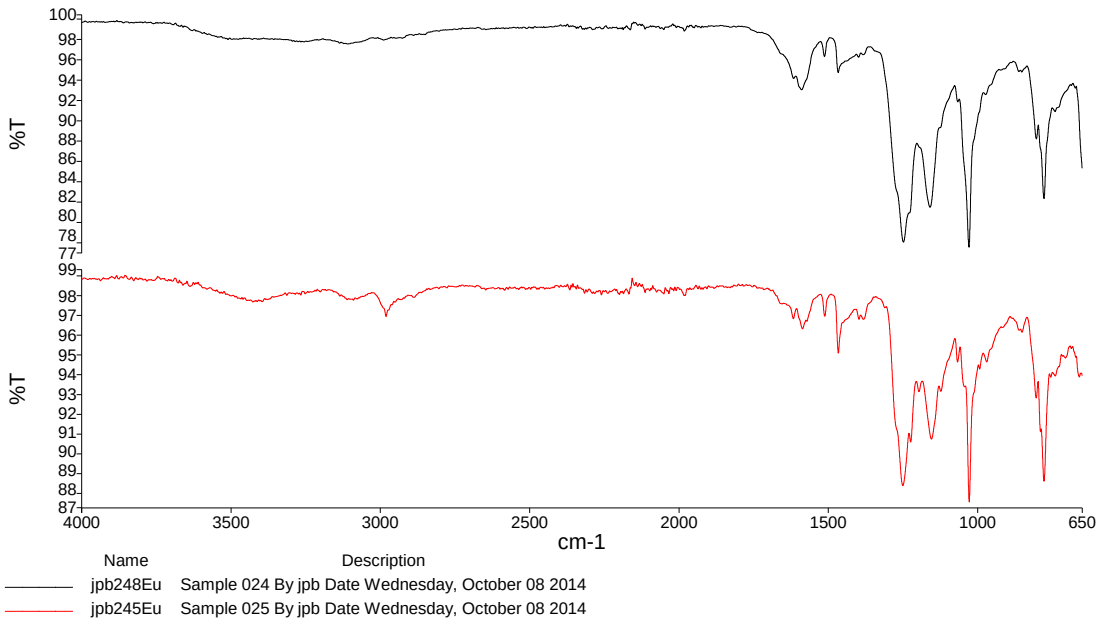

Figure C. 48 IR spectra of Eu(III) complexes of ligands **100b** and **100a**.

C.3. Mass spectrometry of complexes

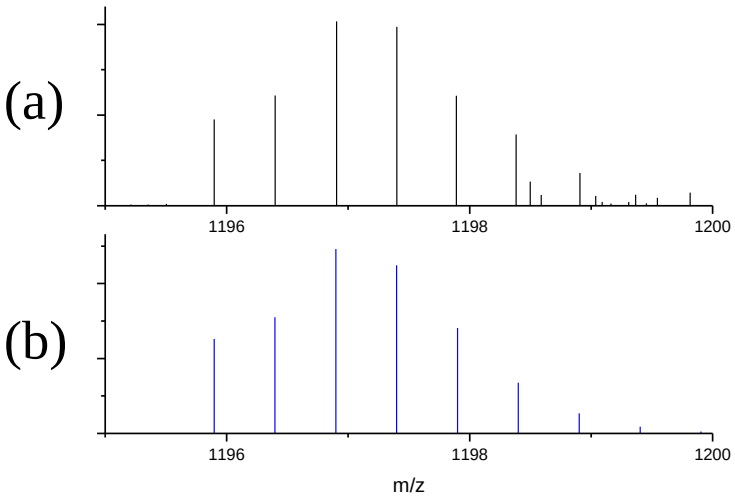

Figure C.49 (a) Experimental and **(b)** calculated HRMS (ESI+) spectra of $[Eu\cdot(\mathbf{96})_3](CF_3SO_3)_3$. Calculated for $C_{100}H_{129}N_{21}O_{33}F_3SEu^{2+}$ *m/z* = 1197.3990 $[EuL_3(CF_3SO_3)]^{2+}$. Found *m/z* = 1197.4003.

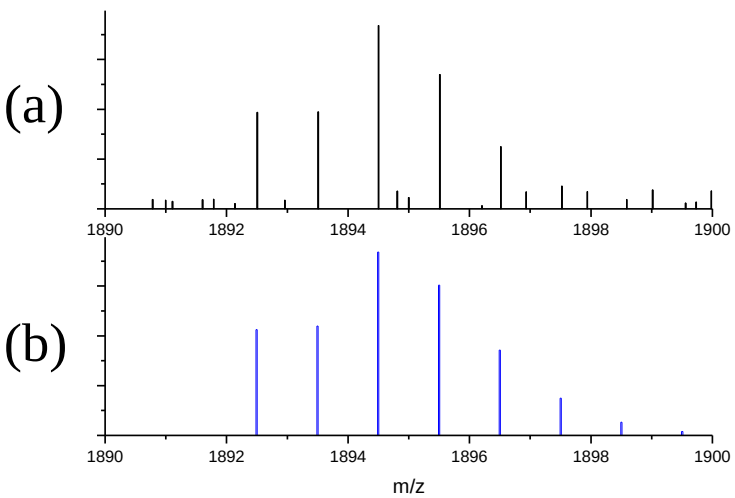

Figure C.50 (a) Experimental and **(b)** calculated HRMS (MALDI+) spectra of $[Eu\cdot(\mathbf{99b})_3](CF_3SO_3)_3$. Calculated for $C_{83}H_{81}N_{21}O_{12}F_6S_2Eu^{+}$ *m/z* = 1894.4932 $[EuL_3(CF_3SO_3)_2]^{+}$. Found *m/z* = 1894.5000

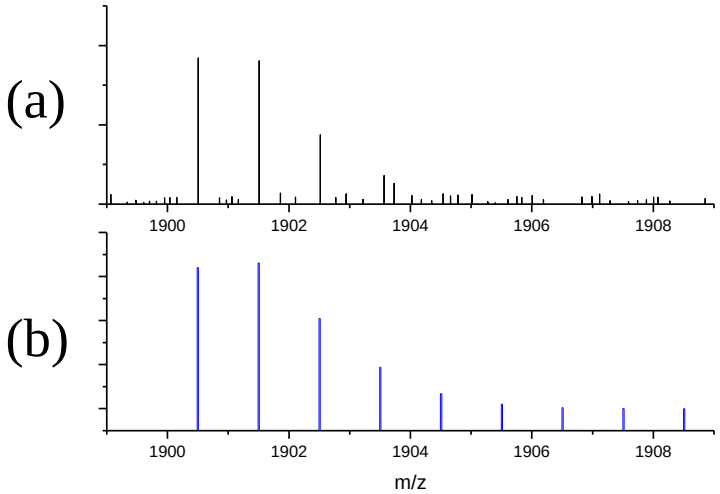

Figure C.51 (a) Experimental and **(b)** calculated HRMS (MALDI+) spectra of [Tb·(**99b**)$_3$](CF$_3$SO$_3$)$_3$. Calculated for $C_{83}H_{81}N_{21}O_{12}F_6S_2Tb^+$ *m/z* = 1900.4973 $[TbL_3(CF_3SO_3)_2]^+$. Found *m/z* = 1900.4973.

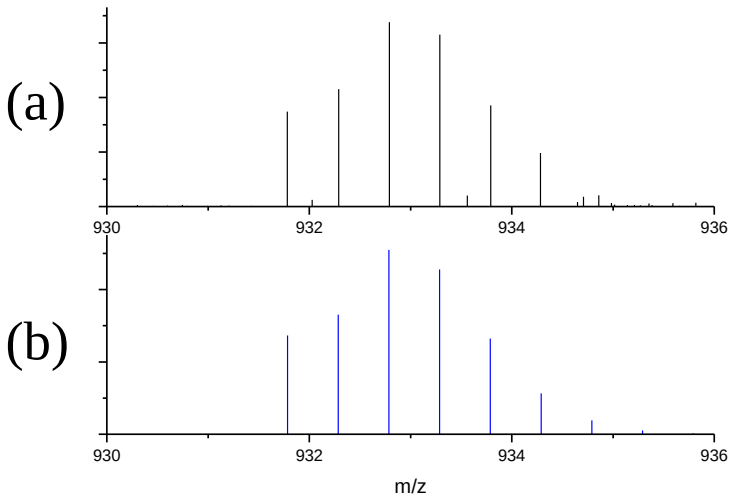

Figure C.52 (a) Experimental and **(b)** calculated HRMS (ESI+) spectra of [Eu·(**100b**)$_3$](CF$_3$SO$_3$)$_3$. Calculated for $C_{100}H_{81}N_{21}O_3F_3SEu^{2+}$ *m/z* = 933.2875 $[EuL_3(CF_3SO_3)]^{2+}$. Found *m/z* = 933.2887.

C.4. X-Ray crystallography

96. When refinement of **96** was finished, the remaining electron density found in the voids of the structure was removed using the SQUEEZE program.

Table C.1 Bond lengths [Å] and angles [°] of supramolecular and non-classical hydrogen bonding interactions in the structure of **98**.

D*—H···*A	***D*—H**	**H···*A***	***D*···*A***	***D*—H···*A***
C8—H8···O17	1.00	2.66	3.572(10)	151.7
C5—H5···N5	0.95	2.61	3.511(10)	157.7
C35—H35B···O7	0.98	2.78	3.545(11)	135.4
C19—H19A···O1	0.98	2.80	3.496(10)	128.4
C19—H19B···N2	0.98	2.59	3.537(11)	163.5
C24—H24···N1	0.95	2.58	3.482(9)	158.1
C38—H38C···O2	0.98	2.78	3.547(12)	135.2
C38—H38B···N6	0.98	2.64	3.363(11)	131.1
C16—H16B···O16	0.98	2.68	3.539(10)	146.7
C16—H16C···O18	0.98	2.74	3.411(12)	126.5
C29—H29···O5	1.00	2.49	3.417(10)	155.0
C31—H31C···O16	0.98	2.66	3.457(12)	138.8
C14—H14A···O4	0.98	2.66	3.540(10)	149.5
C21—H21···O18	0.95	2.48	3.334(12)	149.0

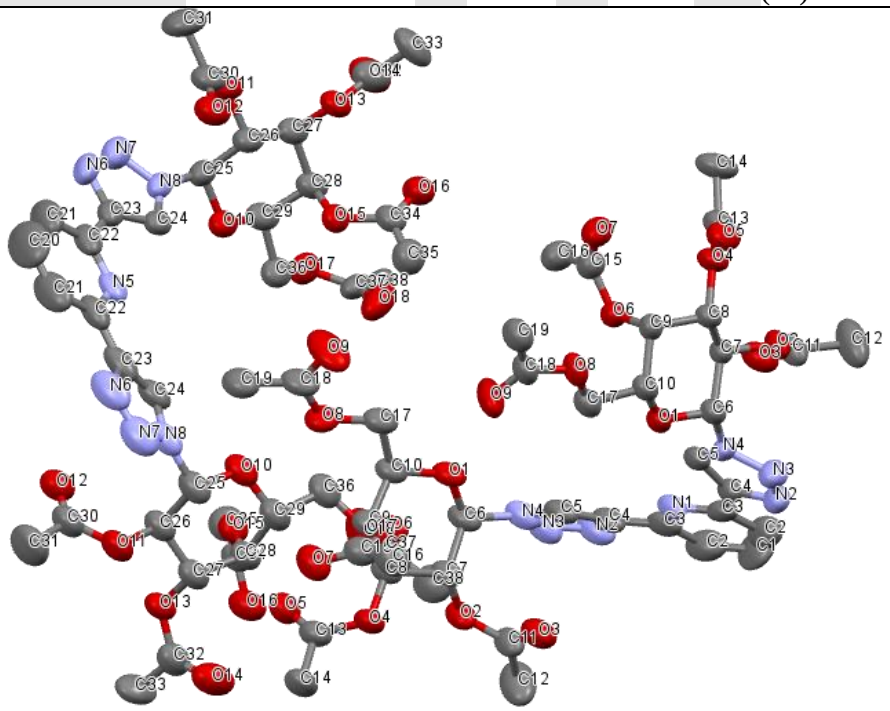

Figure C.53 Ellipsoid plot of the crystal structure of ligand **98**.

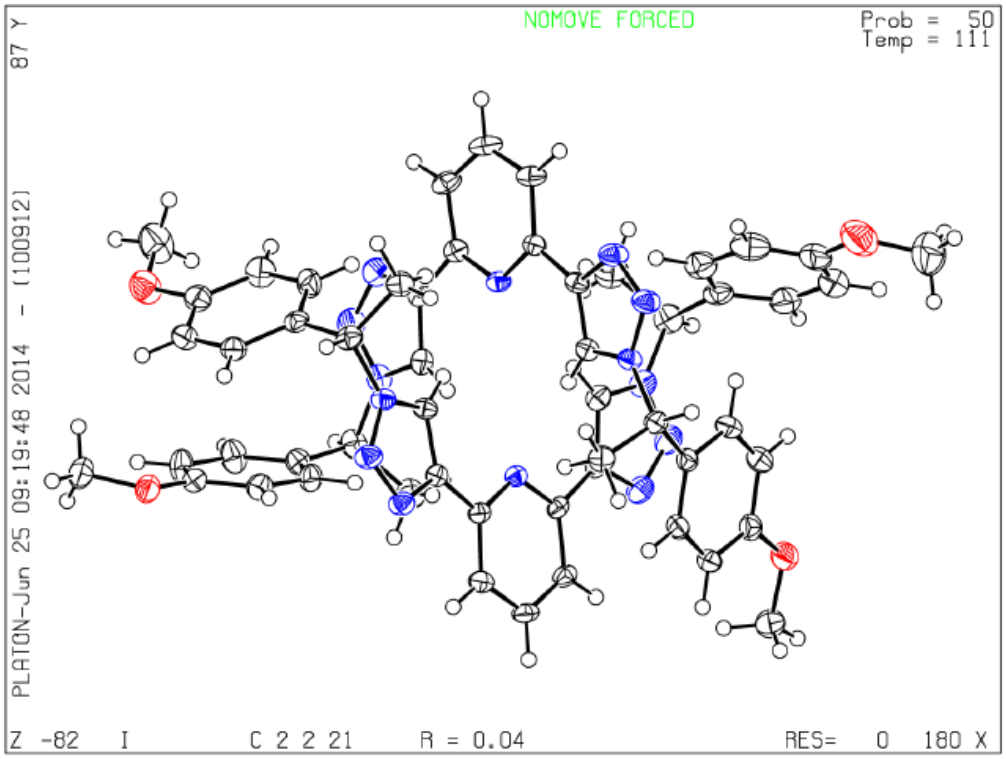

Figure C.54 Ellipsoid plot of the crystal structure of ligand **99a**.

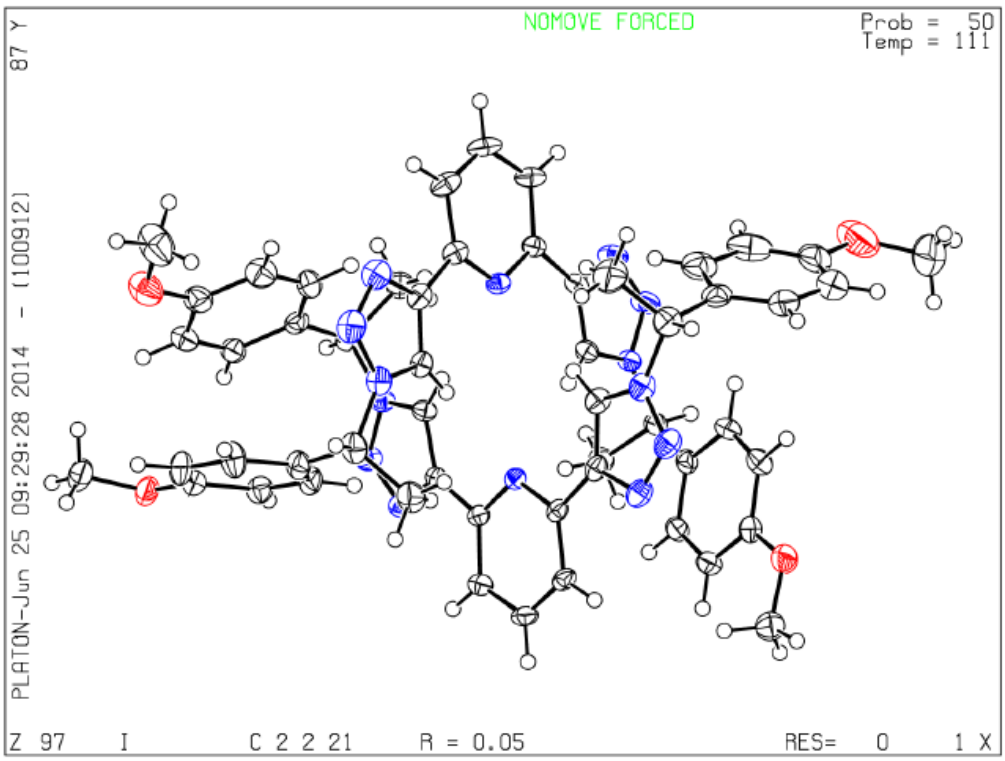

Figure C.55 Ellipsoid plot of the crystal structure of ligand **99b**.

Table C.2 Hydrogen bond lengths [Å] and angles [°] for X-ray crystal structures of **99a** and **99b**.

Ligand	D–H···A	*d*(|D···A|) [Å]	*d*(|H···A|) [Å]	∠(D–H···A) [°]
99a	C(18)–H(18)···N(2)	3.538(2)	2.593(2)	173.6(2)
	C(20)–H(2)···N(2)	3.504(2)	2.562(2)	171.6(2)
	C(35)–H(35)···N(1)	3.537(2)	2.589(2)	175.4(2)
	C(6)–H(6)···N(1)	3.397(2)	2.458(2)	170.1(2)
99b	C(11)–H(11)···N(2)	3.534(3)	2.608(3)	173.7(2)
	C(12)–H(12)···N(2)	3.510(3)	2.588(3)	171.3(2)
	C(7)–H(7)···N(1)	3.532(3)	2.604(3)	175.3(2)
	C(17)–H(17)···N(1)	3.396(3)	2.476(3)	169.9(2)

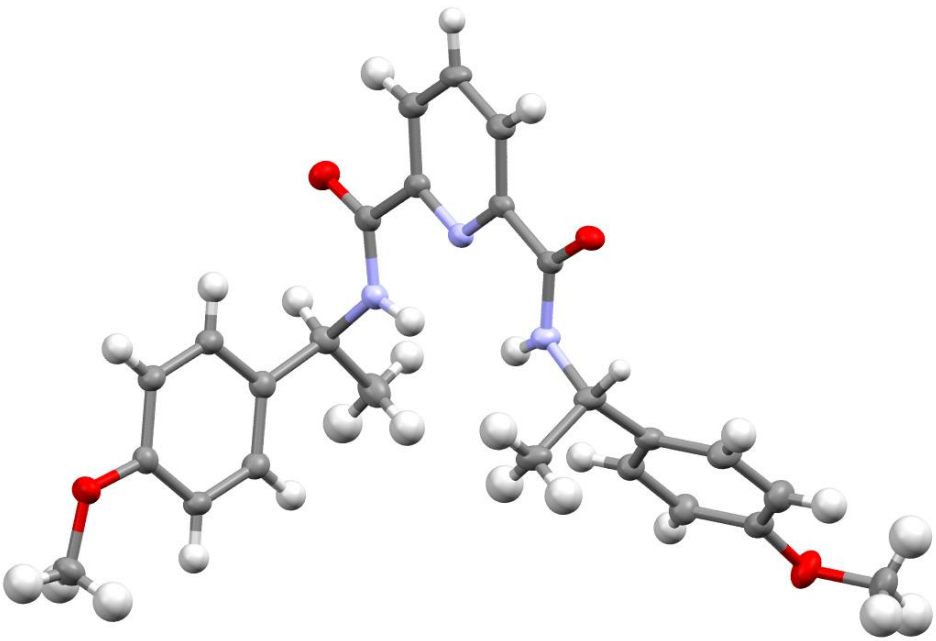

Figure C.56 X-ray crystal structure of ligand **103**.

C.5. Spectroscopic titrations and fitting

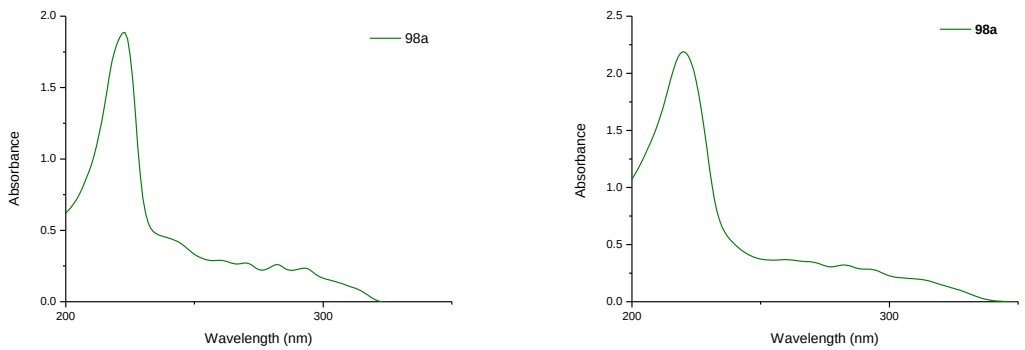

Figure C.57 UV-Vis absorbance spectra of (*left*) **100a**; (*right*) [Eu·(**100a**)$_3$](CF$_3$SO$_3$)$_3$.

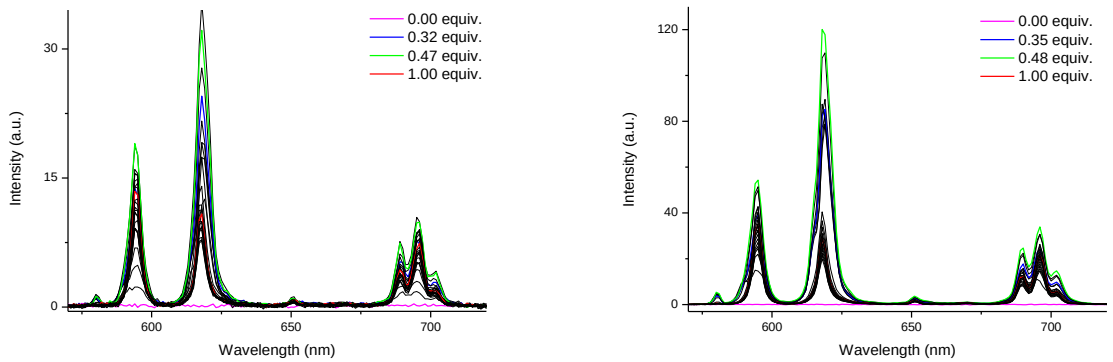

Figure C.58 Phosphorescence emission titrations of ligands **99a** (*left*) and **99b** (*right*) with $Eu(CF_3SO_3)_3$ in CH_3CN, showing characteristic emission bands relating to Eu(III) transitions $^5D_0 \rightarrow {}^7F_J$ (J=0–4). [**99a**]=0.9×10^{-5} M, [**99b**] = 1×10^{-5} M.

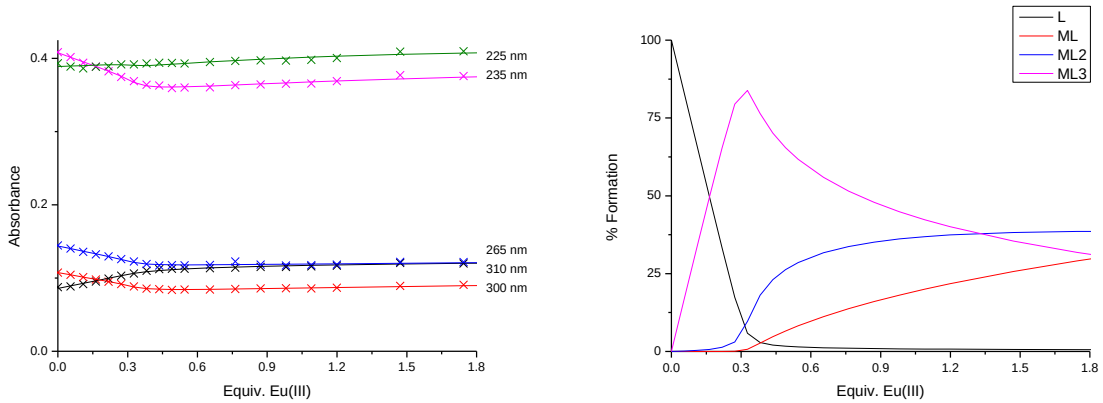

Figure C.59 Titration of ligand **99b** with $Eu(CF_3SO_3)_3$ in CH_3CN: (a) Experimental UV-Vis absorbance binding isotherms (×) and fits (solid lines) calculated using ReactLab Equilibira, at a range of wavelengths and (b) calculated speciation diagram, showing the percentage abundance of the ligand and the various metal:ligand stoichiometries as a function of [Eu(III)].

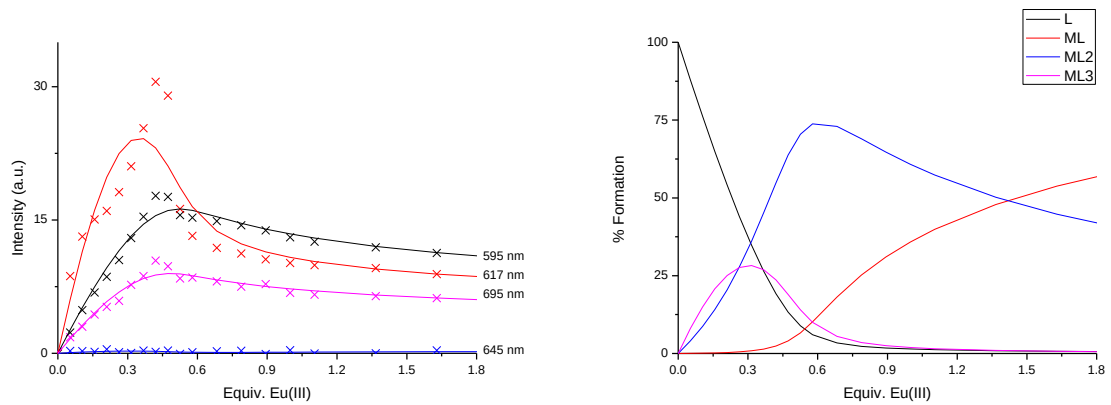

Figure C.60 Titration of ligand **99a** with $Eu(CF_3SO_3)_3$ in CH_3CN: (a) Experimental phosphorescence emission binding isotherms (×) and fits (solid lines) calculated using ReactLab Equilibira, at a range of wavelengths and (b) calculated speciation diagram, showing the percentage abundance of the ligand and the various metal:ligand stoichiometries as a function of [Eu(III)].

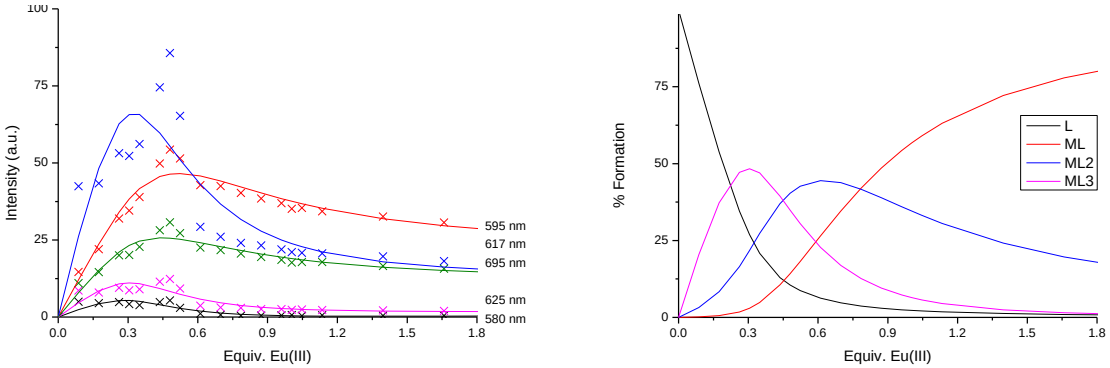

Figure C.61 Titration of ligand **99b** with $Eu(CF_3SO_3)_3$ in CH_3CN: (a) Experimental phosphorescence emission binding isotherms (×) and fits (solid lines) calculated using ReactLab Equilibira, at a range of wavelengths and (b) calculated speciation diagram, showing the percentage abundance of the ligand and the various metal:ligand stoichiometries as a function of [Eu(III)].

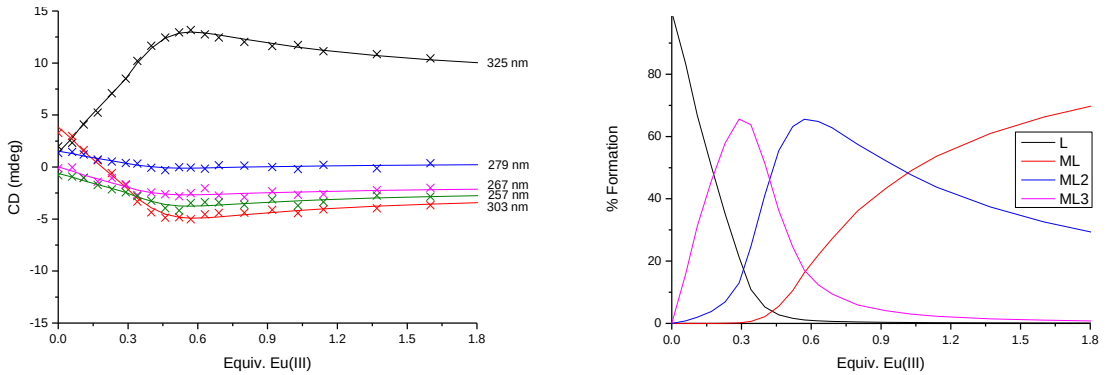

Figure C.62 Titration of ligand **99a** with $Eu(CF_3SO_3)_3$ in CH_3CN: (a) Experimental CD binding isotherms (×) and fits (solid lines) calculated using ReactLab Equilibira, at a range of wavelengths and (b) calculated speciation diagram, showing the percentage abundance of the ligand and the various metal:ligand stoichiometries as a function of [Eu(III)].

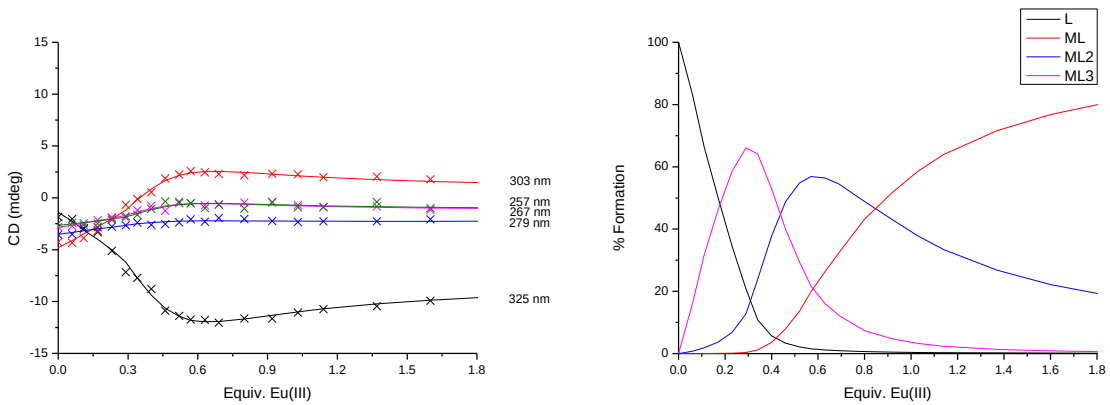

Figure C.63 Titration of ligand **99b** with $Eu(CF_3SO_3)_3$ in CH_3CN: (a) Experimental CD binding isotherms (×) and fits (solid lines) calculated using ReactLab Equilibira, at a range of wavelengths and (b) calculated speciation diagram, showing the percentage abundance of the ligand and the various metal:ligand stoichiometries as a function of [Eu(III)].

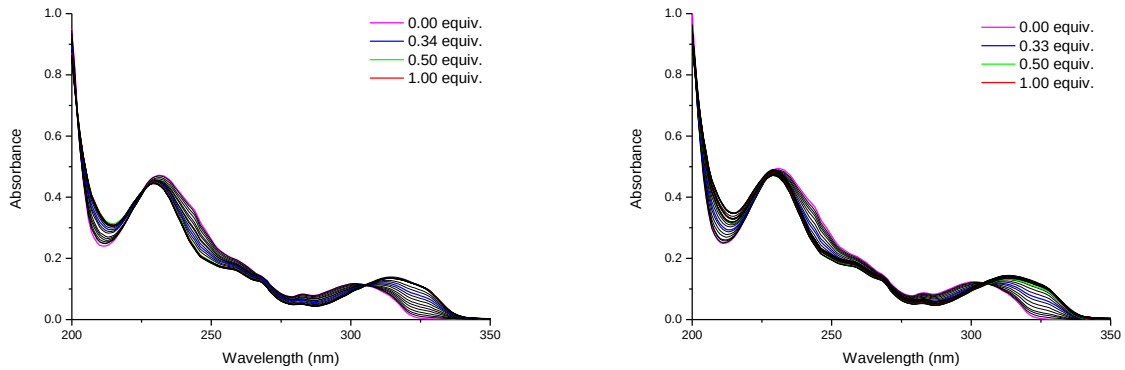

Figure C.64 UV-Vis absorbance titrations of ligands **99a** (*left*) and **99b** (*right*) with $Tb(CF_3SO_3)_3$ in CH_3CN. [**99a**] = 1.0×10^{-5} M, [**99b**] = 1.0×10^{-5} M.

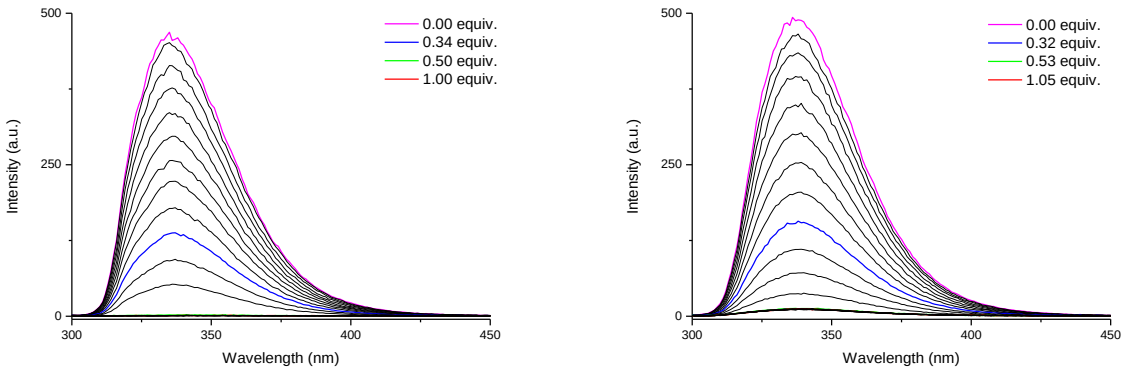

Figure C.65 Fluorescence emission titrations of ligands **99a** (*left*) and **99b** (*right*) with $Tb(CF_3SO_3)_3$ in CH_3CN. [**99a**] = 1.0×10^{-5} M, [**99b**] = 1.0×10^{-5} M.

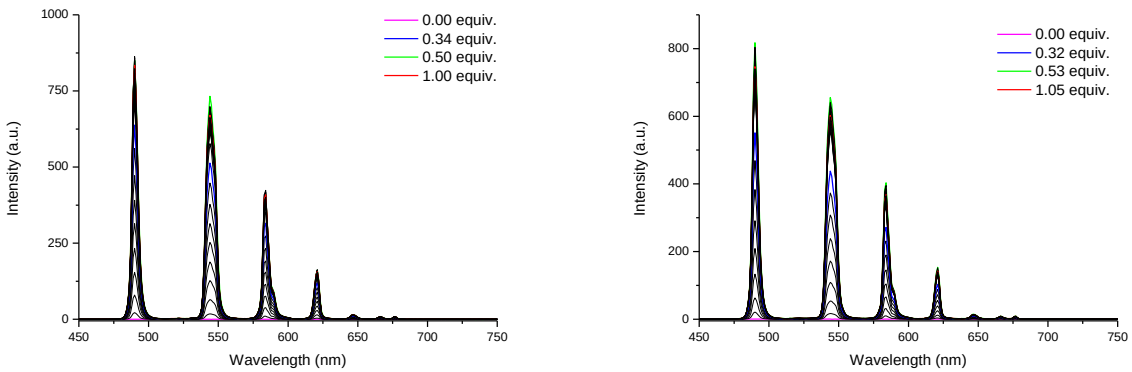

Figure C.66 Phosphorescence emission titrations of ligands **99a** (*left*) and **99b** (*right*) with $Tb(CF_3SO_3)_3$ in CH_3CN, showing characteristic emission bands relating to Tb(III) transitions $^5D_4 \rightarrow {}^7F_J$ (J=6–0). [**99a**] = 1.0×10^{-5} M, [**99b**] = 1.0×10^{-5} M.

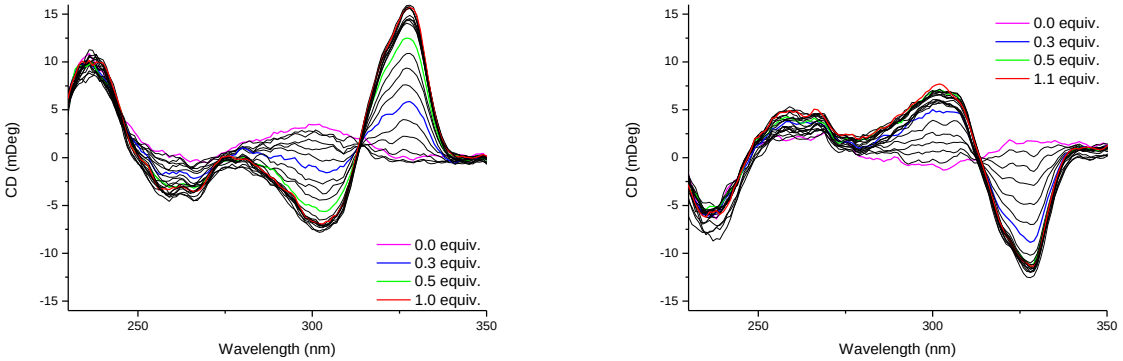

Figure C.67 CD Titrations of ligands **99a** (*left*) and **99b** (*right*) with $Tb(CF_3SO_3)_3$ in CH_3CN. [**99a**] = 1.3×10^{-5} M, [**99b**] = 1.4×10^{-5} M.

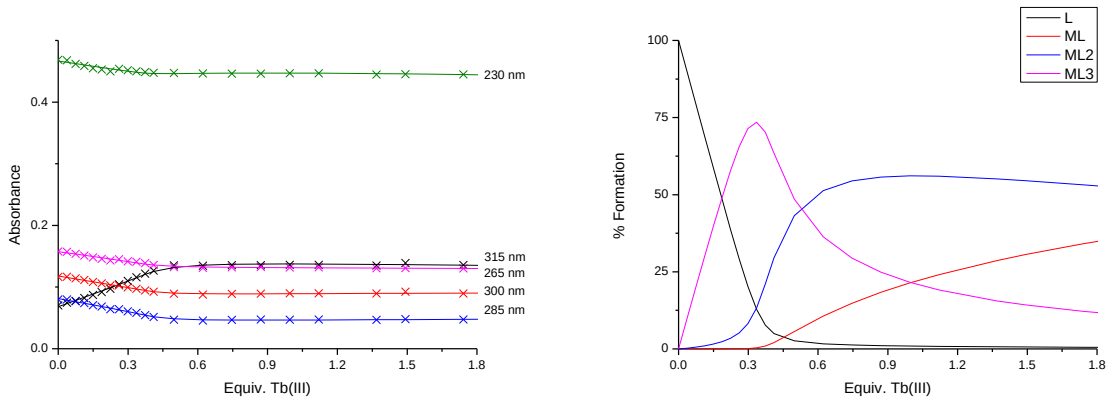

Figure C.68 Titration of ligand **99a** with $Tb(CF_3SO_3)_3$ in CH_3CN: (a) Experimental UV-Vis absorbance binding isotherms (×) and fits (solid lines) calculated using ReactLab Equilibira, at a range of wavelengths and (b) calculated speciation diagram, showing the percentage abundance of the ligand and the various metal:ligand stoichiometries as a function of [Tb(III)].

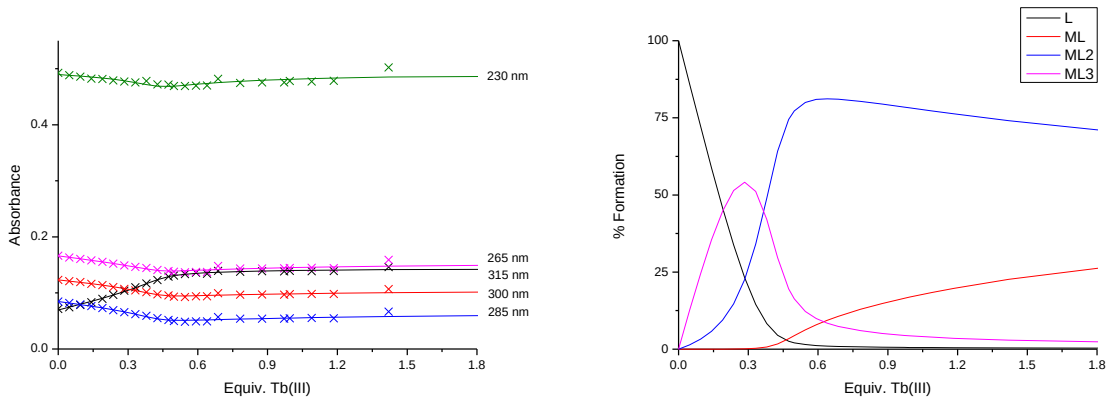

Figure C.69 Titration of ligand **99b** with $Tb(CF_3SO_3)_3$ in CH_3CN: (a) Experimental UV-Vis absorbance binding isotherms (×) and fits (solid lines) calculated using ReactLab Equilibira, at a range of wavelengths and (b) calculated speciation diagram, showing the percentage abundance of the ligand and the various metal:ligand stoichiometries as a function of [Tb(III)].

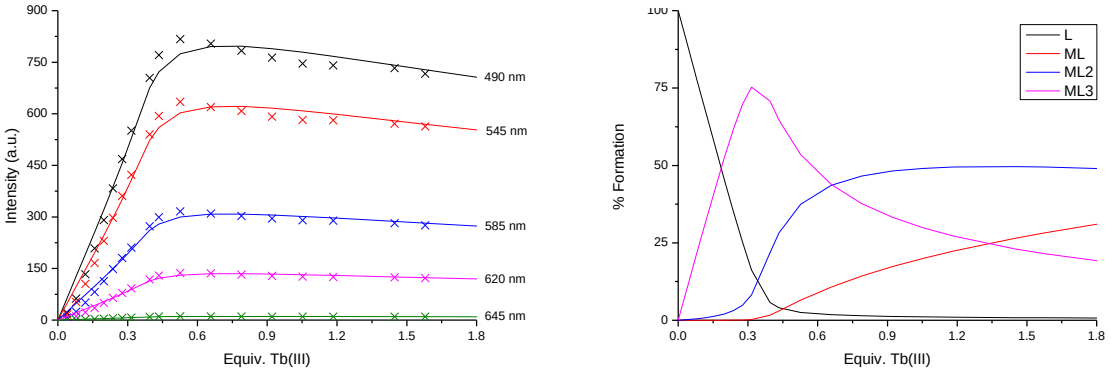

Figure C.70 Titration of ligand **99b** with $Tb(CF_3SO_3)_3$ in CH_3CN: (a) Experimental phosphorescence emission binding isotherms (×) and fits (solid lines) calculated using ReactLab Equilibira, at a range of wavelengths and (b) calculated speciation diagram, showing the percentage abundance of the ligand and the various metal:ligand stoichiometries as a function of [Tb(III)].

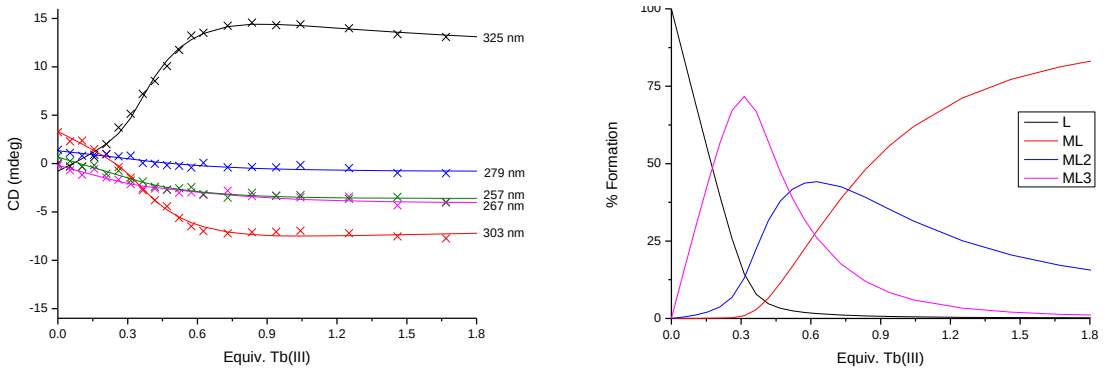

Figure C.71 Titration of ligand **99a** with $Tb(CF_3SO_3)_3$ in CH_3CN: (a) Experimental CD binding isotherms (×) and fits (solid lines) calculated using ReactLab Equilibira, at a range of wavelengths and (b) calculated speciation diagram, showing the percentage abundance of the ligand and the various metal:ligand stoichiometries as a function of [Tb(III)].

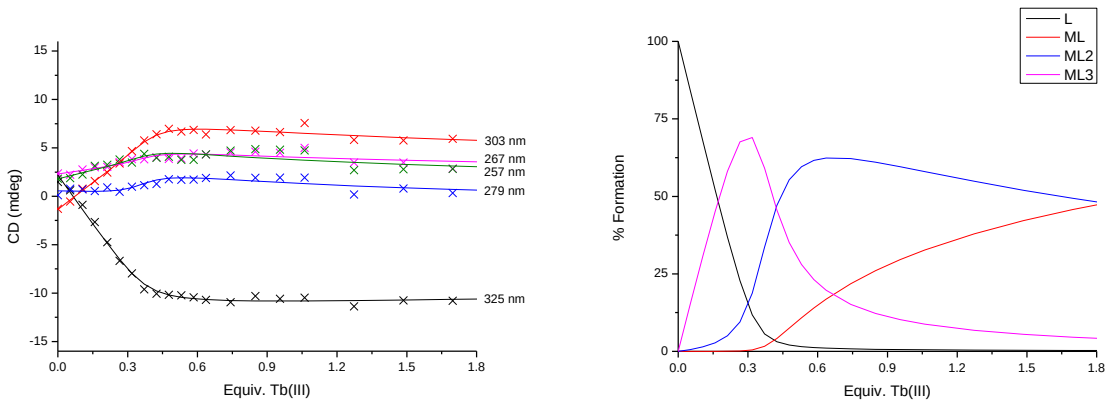

Figure C.72 Titration of ligand **99b** with $Tb(CF_3SO_3)_3$ in CH_3CN: (a) Experimental CD binding isotherms (×) and fits (solid lines) calculated using ReactLab Equilibira, at a range of wavelengths and (b) calculated speciation diagram, showing the percentage abundance of the ligand and the various metal:ligand stoichiometries as a function of [Tb(III)].

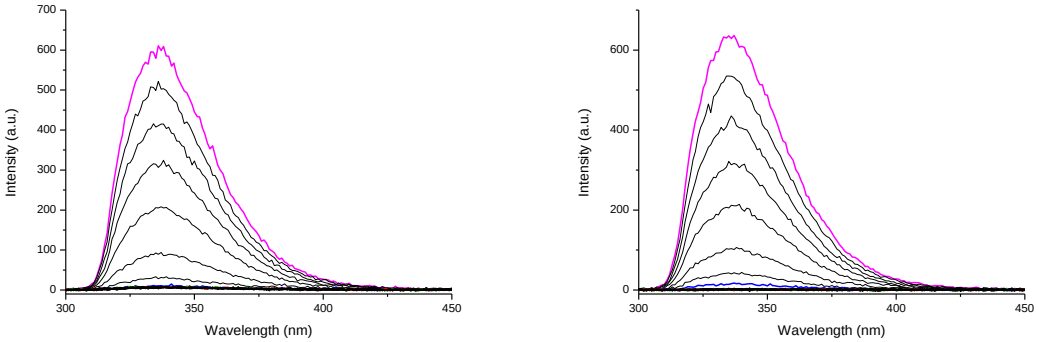

Figure C.73 Fluorescence emission titrations of ligands **100a** (*left*) and **100b** (*right*) with $Eu(CF_3SO_3)_3$ in CH_3CN. [**100a**] = 1×10^{-5} M, [**100b**] = 1.1×10^{-5} M.

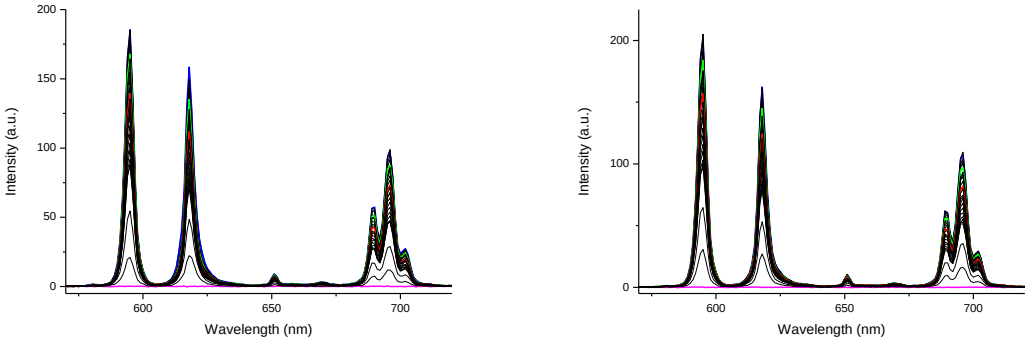

Figure C.74 Eu(III)-centred phosphorescence emission titrations of ligands **100a** (*left*) and **100b** (*right*) with $Eu(CF_3SO_3)_3$ in CH_3CN, showing characteristic emission bands relating to Eu(III) transitions $^5D_0 \rightarrow {}^7F_J$ (J=1–4). [**100**]=1.1×10^{-5} M, in both cases.

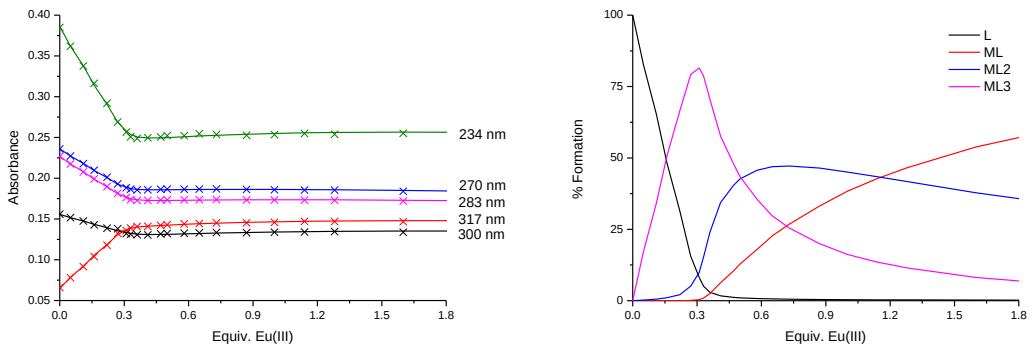

Figure C.75 Titration of ligand **100b** with $Eu(CF_3SO_3)_3$ in CH_3CN: **(a)** Experimental UV-Vis absorbance binding isotherms (×) and fits (solid lines) calculated using ReactLab Equilibira, at a range of wavelengths and **(b)** calculated speciation diagram, showing the percentage abundance of the ligand and the various metal:ligand stoichiometries as a function of [Eu(III)].

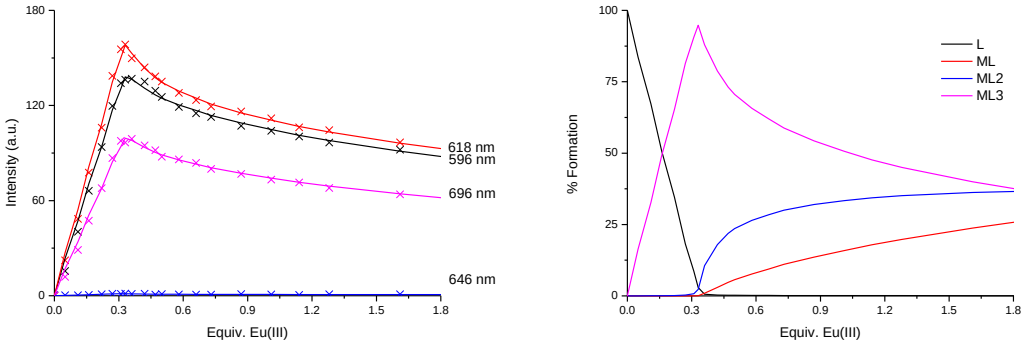

Figure C.76 Titration of ligand **100a** with $Eu(CF_3SO_3)_3$ in CH_3CN: **(a)** Experimental Eu(III)-centred luminescence binding isotherms (×) and fits (solid lines) calculated using ReactLab Equilibira, at a range of wavelengths and **(b)** calculated speciation diagram, showing the percentage abundance of the ligand and the various metal:ligand stoichiometries as a function of [Eu(III)].

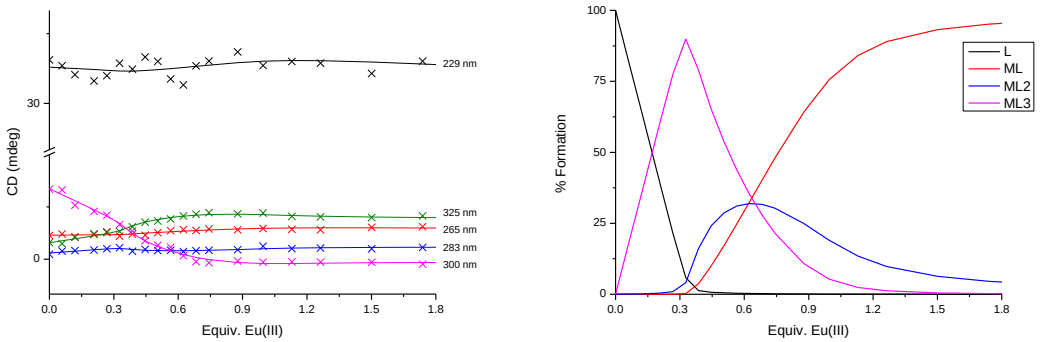

Figure C.77 Titration of ligand **100a** with $Eu(CF_3SO_3)_3$ in CH_3CN: **(a)** Experimental CD binding isotherms (×) and fits (solid lines) calculated using ReactLab Equilibira, at a range of wavelengths and **(b)** calculated speciation diagram, showing the percentage abundance of the ligand and the various metal:ligand stoichiometries as a function of [Eu(III)].

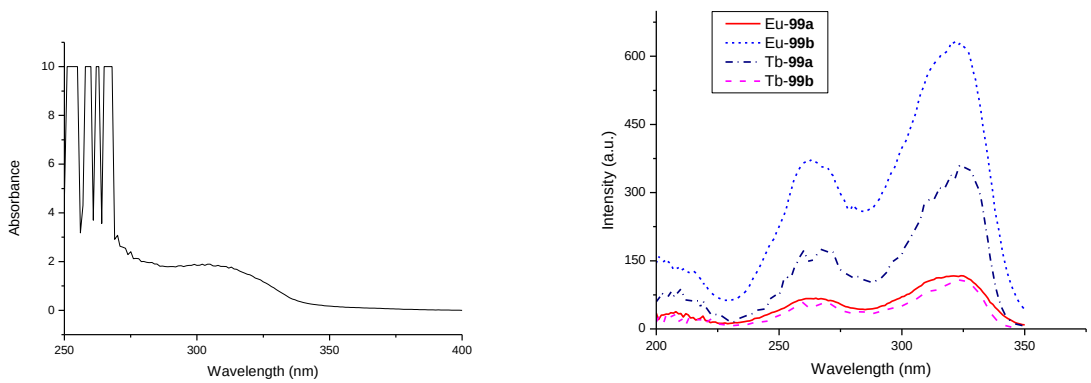

Figure C.78 Photophysical spectra of Ln(III)-swelled cross-linked poly(HEMA) hydrogels with **99** encapsulated: *(left)*: UV-Vis absorbance spectrum of Tb(III)-swelled gel encapsulating **99b**; *(right)*: Excitation spectra of Ln(III)-centred emission for all gels.

Publications